Chapter 1. Introduction

Trickle flow is encountered in packed beds of stationary particles that are subjected to co-current gas and liquid flow at relatively low fluid superficial velocities. Typical applications where trickle flow may be encountered are trickle bed reactors, catalytic distillation columns, trickling filters and absorption columns.

The study of trickle flow hydrodynamics has been the subject of a multitude of research works over the last five decades. Sadly, a rigorous and fundamentally exhaustive mathematical description of trickle flow dynamics has not yet been achieved. Owing to the difficulties involved in modelling the complexities of three inter-acting phases, it seems that such a fundamental description is unlikely to be developed in the foreseeable future. However, as will be seen from the subsequent chapter, significant progress towards this goal has been made, especially with regards to obtaining phenomenological (semi-empirical) models that capture hydrodynamic trends with reasonable degrees of accuracy. Nevertheless, these models nearly always disagree quantitatively and the level of accuracy is often insufficient to inspire confidence in using their predictions for design purposes. It is for this reason that most authors recommend incorporating as much of the underlying physics as possible into any hydrodynamic investigation.

Hydrodynamics is quantified in terms of *hydrodynamic parameters* (like pressure drop and liquid holdup) that are related in some way to the gas-liquid-solid contacting effectiveness and the operational efficiency of the reactor or column. A phenomenon that greatly complicates the mathematical description of trickle flow hydrodynamics is the fact that these hydrodynamic parameters are path-variables (which are dependent on the history of operation) as opposed to state-variables (which depend only on the present operating conditions). This phenomenon manifests itself in the form of hysteresis loops or multiple hydrodynamic states – in this work these are collectively referred to as

hydrodynamic multiplicity. Although the existence of multiplicity was recognized as early as 1978 (Kan & Greenfield, 1978), it has generally not featured in hydrodynamic models. For example, in their respective comprehensive reviews, Gianetto & Specchia (1992), Larachi et al. (2000), Dudukovic et al. (2002) and Kundu et al. (2003) recommend numerous pressure drop and liquid holdup correlations – none of which incorporate the existence of hydrodynamic multiplicity.

This work addresses the issue of trickle flow hydrodynamic multiplicity. The main objective is to identify the fundamental mechanism behind the observed behaviour. The strategy that was followed to achieve this is outlined in Figure 1. The figure also provides a handy guide to the structure of this thesis as every major chapter directly addresses one or more of the blocks in this figure.

The first step is to critically evaluate previous work in this field. Since any of the hydrodynamic parameters can take on a continuum of values, it is necessary to establish a framework by which the phenomenon can be understood conceptually and studied experimentally. The proposed framework makes it possible to re-interpret the literature and thereby identify issues that need to be addresses experimentally. Experimental investigations therefore form the next major part of this work. This is done both at the bed-scale (macro) and the cluster-of-particles scale (meso). The re-interpretation of the literature and the experimental results makes it possible to compile a list of trends that are the characteristic manifestations of hydrodynamic multiplicity. These characteristic trends then lead to the identification of the controlling physical mechanism that is responsible for the existence of hydrodynamic multiplicity. The trends also set the benchmark by which multiplicity should be modelled.

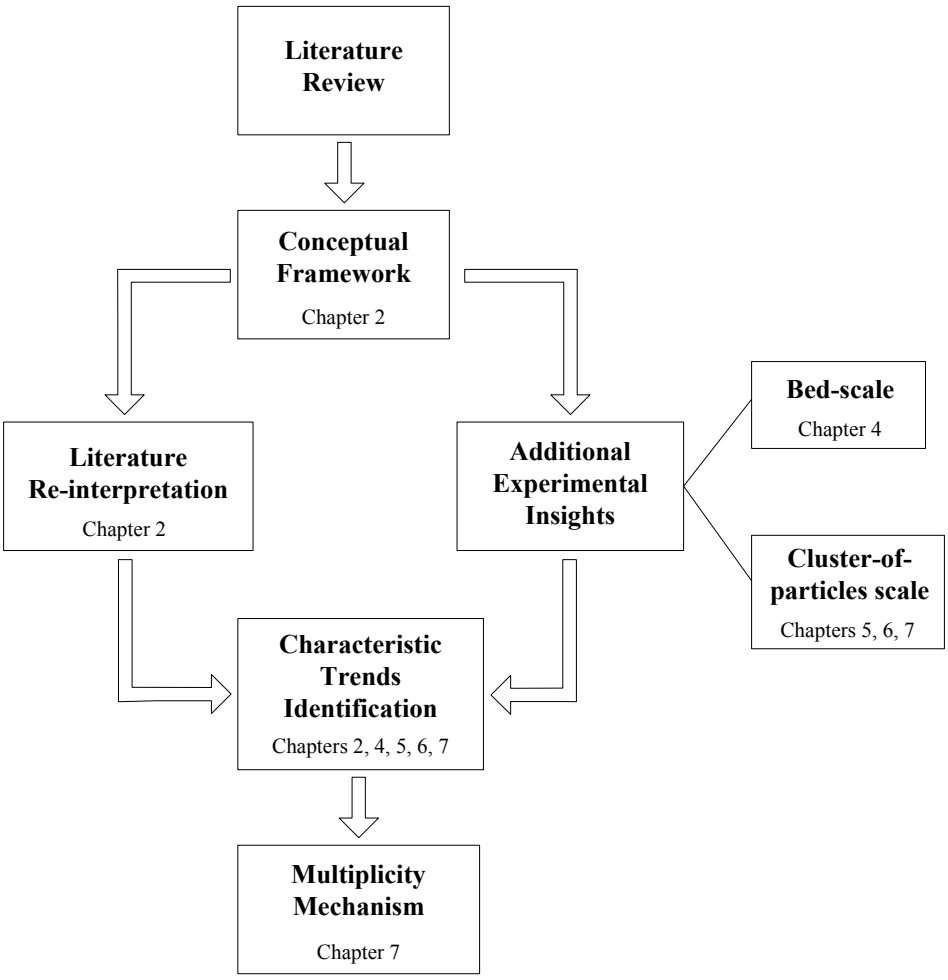

Figure 1. Schematic of the structure of this work.

To round off the work, a final chapter explores the implications of hydrodynamic multiplicity for the typical operation of a trickle bed reactor (both theoretically and experimentally). The novel idea of using hydrodynamic multiplicity to optimize the reactor performance based on the characteristics of the reaction system is introduced.

It is the purpose of this work to advance the fundamental understanding of trickle flow hydrodynamics in general and hydrodynamic multiplicity in particular.

Chapter 2. Literature

This chapter reviews the results of previous hydrodynamic multiplicity studies (Literature Review block in Figure 1). On the basis of the results of these studies a conceptual framework is introduced (Conceptual Framework block) and the literature is re-interpreted in terms thereof (Literature Re-interpretation block). The chapter concludes with listing those characteristic multiplicity trends that can be extracted from literature (part of the Characteristic Trends Identification block in Figure 1). Note that this follows the investigative strategy set out in Figure 1.

There is a large body of literature dedicated to trickle flow hydrodynamics in general and an in-depth review of each study would be superfluous. The reader is referred to several review articles (Satterfield, 1975, Gianetto et al., 1978, Al-Dahhan et al., 1997, Dudukovic et al., 2002, Sie & Krishna, 1998, Kundu et al., 2003). Instead, the scope of this chapter is limited to presenting only the information that is pertinent to the discussion of hydrodynamic multiplicity. In addition, relevant information from multiple sources are summarized into tables where possible. The first section of this chapter deals with definitions and hydrodynamic concepts in general. The second section reviews experimental investigations into hydrodynamic multiplicity and identifies issues that need further experimental clarification. The third section first summarizes the common approaches adopted to model general trickle flow hydrodynamics and then reviews the existing proposals to incorporate multiplicity into hydrodynamic models. This section also includes a critical evaluation of the potential of existing modelling approaches to be extended to include hydrodynamic multiplicity.

2.1 Trickle Flow Hydrodynamics in General

Trickle flow hydrodynamics are studied by measuring hydrodynamic parameters that are linked in some way to the performance of the trickle flow column. Definitions of the most commonly encountered hydrodynamic parameters are given in Table 1. Note that non-isothermal effects are not included in this work, except briefly in connection with the reaction case study reported in Chapter 8.

Table 1. Definitions of hydrodynamic parameters

Parameter	**Notation**	**Definition**
Liquid holdup (liquid saturation)	ε_L (β_L)	Volume of liquid in the bed as a fraction of the total bed volume (volume of liquid as a fraction of the void volume).
Pressure drop	$\left(\frac{\Delta P}{\Delta z}\right)$	Two-phase pressure drop per unit bed length.
Wetting efficiency	f	The fraction of the external solid surface area that is wetted by the liquid.
Gas-liquid mass transfer coefficient	$k_{GL}a_{GL}$	Volumetric gas-liquid mass transfer coefficient. Note that it includes the specific gas-liquid area, primarily because it is difficult to measure the area independently.
Liquid-solid mass transfer coefficient	$k_{LS}a_{LS}$	Volumetric liquid-solid mass transfer coefficient (including the liquid-solid mass transfer area).
Liquid phase axial dispersion	D_{AX}	A measure of the mixedness of the liquid phase obtained from residence time distribution analysis.
Liquid maldistribution factor	M	A measure of the cross-sectional distribution of the liquid in the bed. The exact definition depends on the application.

Table 2 is a summary of the methods by which these parameters are evaluated experimentally. It also includes order-of-magnitude estimates for each parameter as typically encountered in the trickle regime in trickle bed reactors. The different hydrodynamic parameters influence the column's performance as summarized qualitatively in Table 3 (more detail given in context in Chapter 8). The impact is

potentially large and provides a motivation for the study of hydrodynamics. The purpose of any trickle flow unit is to achieve optimal interaction between the gas, liquid and solid phases. For different applications the degrees of optimal interaction between the phases may be different. For example, in a gas-liquid packed absorption column, the key operational parameter is the volumetric gas-liquid mass transfer coefficient. A high degree of gas-liquid interaction is therefore desirable. On the other hand, in a liquid-limited trickle bed reactor, external and internal liquid phase reactant mass transfer rates will likely be more important.

Table 2. Experimental methods by which parameters are determined

Parameter	**Method(s) of determination**	**Approximate range**
Liquid holdup	Gravimetry (weighing) Mean residence time (tracer methods) Radiography Tomography	0.01 – 0.3
Pressure drop	Differential pressure transducer	0.1 – 20 kPa/m
Wetting efficiency	Residence time distribution analysis Colorimetry Physical methods (force balance)	0.2 – 1.0
Gas-liquid mass transfer coefficient	Physical desorption	10^{-2} – 10^{0} s^{-1}
Liquid solid mass transfer coefficient	Dissolution techniques Electro-chemical probe	10^{-2} – 10^{0} s^{-1}
Liquid phase axial dispersion	Residence time distribution analysis	10^{-4} – 10^{-2} m^2/s
Liquid maldistribution factor	Annular collector Radiography Tomography	Only relative values are meaningful

Composed from: Saez & Carbonell (1985), Al-Dahhan & Dudukovic (1995), Nemec et al. (2001), Al-Dahhan et al. (2000), Kundu et al. (2003), Marcandelli et al. (2000), Basavaraj et al. (2005), Colombo et al. (1976), Goto & Smith (1975), Piche et al. (2002), Satterfield (1975), Dudukovic et al. (2002), Sederman & Gladden (2001).

Table 3. Impact of hydrodynamics on reactor/column performance

Parameter	Impacts performance as follows:
Liquid holdup	Roughly indicative of the liquid-solid contacting efficiency. High holdup also indicates good radial spreading of liquid and large mass transfer areas. Possibly impacts the extent of homogeneous side reactions.
Pressure drop	Indicative of the overall operating cost (the gas recycle compression is often a main operating cost driver). Sometimes taken as indication of the degree of gas-liquid interaction.
Wetting efficiency	Proportional to the external liquid-solid mass transfer area. Also impacts the particle effectiveness. Different effects in gas- and liquid limited reactions.
Gas-liquid mass transfer coefficient	Potential rate limiting step in applications where gas-liquid mass transfer is critical (for example gas-limited reactions and absorption columns).
Liquid solid mass transfer coefficient	Potential rate limiting step for liquid-limited reactions.
Liquid phase axial dispersion	Significant deviation from plug-flow reduces performance. Also related to the wetting efficiency.
Liquid maldistribution factor	Potentially impacts bed utilization (i.e. some catalyst particles may be completely inactive or catalysing gas phase reactions).

Evaluated from: Satterfield (1975), Dudukovic (1977), Beaudry et al. (1987), Gianetto et al. (1978), Nijhuis et al. (2003), Rajashekharam et al. (1998), Wu et al. (1996), Kan & Greenfield (1978).

2.1.1 Flow Regimes

Co-current gas-liquid flow in packed beds adopts a variety of flow morphologies depending on the bed properties and the operating conditions (Gianetto & Specchia 1992). This has historically been illustrated in the form of a flow chart (Charpentier et al., 1969), as shown in Figure 2. Also shown in Figure 2 are schematic snap-shots of the morphologies in the different flow regimes. Hydrodynamic multiplicity occurs only in the trickle and transition regimes (red shaded area) and the focus will be exclusively on these. Figure 3 indicates the operating regions of 58 of the most recently published studies on trickle bed reactors. Although most of these were performed at laboratory or pilot scale, the trickle and transition regimes are clearly important. The pulsing flow regime has significantly higher pressure drops and volumetric gas-liquid and liquid-solid

mass transfer rates than the trickle regime. Reactors are often operated close to the trickle-to-pulse flow boundary because a good balance between high mass transfer rates (effectiveness) and pressure drop (operating efficiency) is achieved here (an example being oil hydroprocessing, Sie & Krishna, 1998).

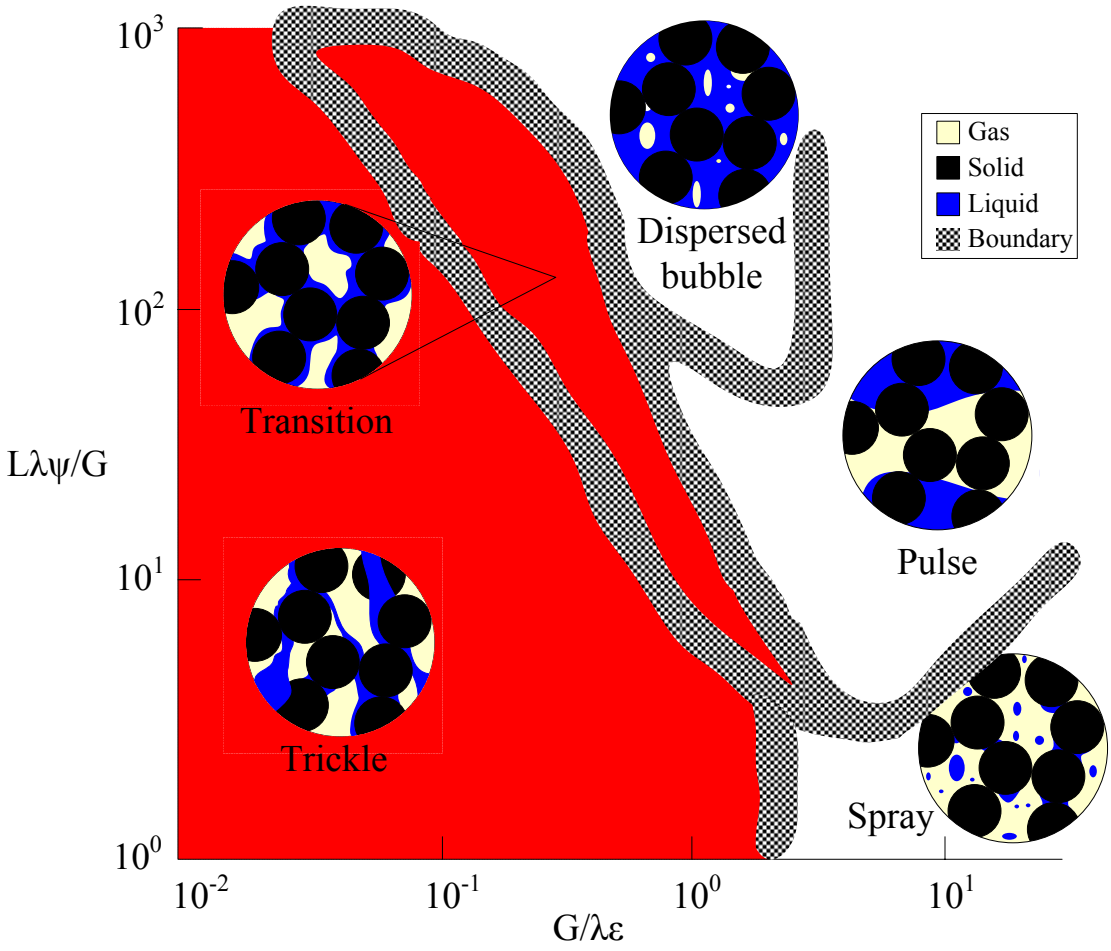

Figure 2. A flow regime map showing the different flow morphologies – the red shaded area shows the regimes where multiplicity exists (based on Charpentier & Favier, 1975, with adaptations from Gianetto et al., 1992, Satterfield, 1975, Sie & Krishna, 1998 and Larachi et al., 1999)

In the pulse, bubble and spray regimes, the flow pattern is transient, while Anadon et al. (2004) has shown that local high frequency instabilities exist in the transition regime. No systematic study of the stability of the flow pattern in the trickle flow regime has been reported, although Kan & Greenfield (1978) and Christensen et al. (1986) report that in

their studies the flow pattern remained stable for at least 24 hours and 2 hours respectively (see Chapter 5).

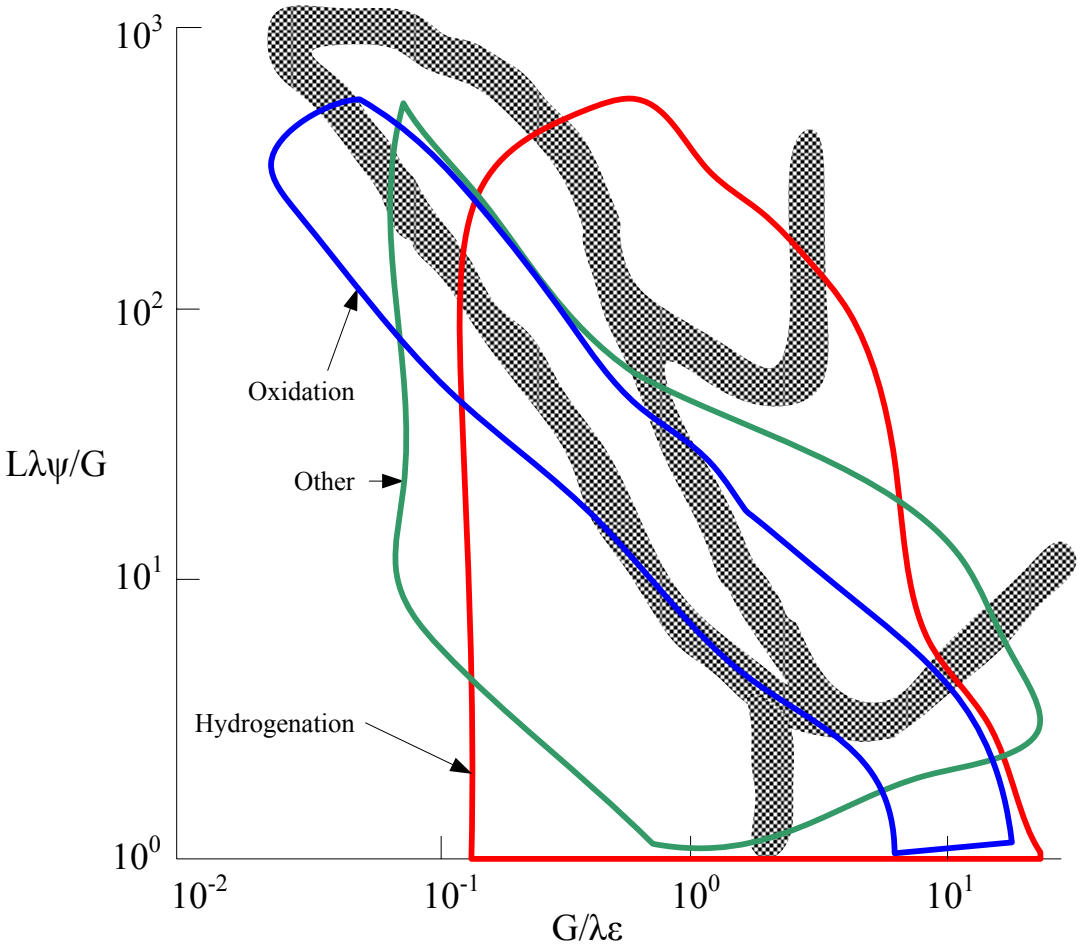

Figure 3. A flow regime map showing the operating velocity ranges of 58 recent trickle bed reactor studies

2.1.2 Hydrodynamic Trends (not associated with multiplicity)

An exhaustive database of experimental data on holdup and pressure drop is now available in literature. From these published results it is possible to qualitatively evaluate the effects of various system and operating conditions on these two hydrodynamic parameters. Table 4 is a form of an inter-connectedness diagram (after Kundu et al., 2003) showing how certain conditions affect the hydrodynamic parameters.

Table 4. Qualitative effect of bed and operating conditions on trickle flow hydrodynamics (based on experimental data)

Bed or Operating Condition	Holdup	Pressure drop	G-L mass transfer	L-S mass transfer	Wetting efficiency	Axial dispersion	Maldistribution factor
Porosity	↓	↓	↑	↑	↓	↑	↓
Particle size	↓	↓	↓	↓	↓	↑	↑
Liquid density	–	↑	↓	?	↓	–	–
Liquid viscosity	↑	↑	↑	?	↑	↓	?
Surface tension	–	↑	↓	?	↓	?	↓
Liquid superficial velocity	↑	↑	↑	↑	↑	↑	↓
Gas superficial velocity	↓	↑	↑	↑	↑	–	↓
Gas viscosity	↑	↑	↑	?	↑	–	?
Pressure (gas density)	↓	↑	↑	↓	↑	?	↓

Composed using data from: Kundu et al. (2003), Larachi et al. (1999), Al-Dahhan & Dudukovic (1995), Al-Dahhan et al. (1997), Lakota & Levec (1990), Saroha et al. (1998), Wang et al. (1999), Piche et al. (2002), Dudukovic et al. (2002).

This table has been compiled from reported trends in the references cited at the end of the table. In rare instances, contradictory trends were reported and the more commonly accepted one is shown in the table. Green arrows indicate that an increase in the operating condition (first column) results in an increase in the hydrodynamic parameter. Red arrows and yellow bars indicate an inverse relation and a negligible effect respectively. A question mark indicates that there is no conclusive data. For example, examining the first row of this table we see that increasing the bed porosity decreases the holdup (first row,

second column), but increases the axial dispersion coefficient (first row, seventh column). This table excludes a few issues that bear mentioning:

- It is desirable is to have the *bed diameter to particle diameter ratio* larger than 25 (Prchlik et al., 1975) or 20 (Sie & Krishna, 1998) in order to avoid the fact that wall-flow effects alter the bed-averaged parameter values. This is difficult to achieve in practice (Al-Dahhan et al., 1995b) and other authors have suggested that values between 12 and 18 are satisfactory (Gierman, 1988, Herskowitz & Smith, 1983). For single phase flow a value of 10 is considered sufficient (Nemec & Levec, 2005a).
- *Bed height* similarly influences the hydrodynamics only if too short a bed is used. However, if a uniform liquid distributor is used at the top of the bed, a bed length larger than 200 mm ensures that entrance effects are negligible (using the correlation in Gianetto et al., 1992 for typical trickle flow conditions).
- More than one *packing method* exist (including sock, dense and loose loading). However, there is little evidence that it impacts the hydrodynamics apart from its effect on bed porosity. Nemec et al. (2005b) recently showed that the *shape of the particles* (spheres, cylinders, extrudate) has little effect on the hydrodynamics, except when hollow cylinders are used. Larachi et al. (1999) incorporated a sphericity factor into their artificial neural network equations. Keeping all other operating variables constant (including effective diameter), both pressure drop and liquid holdup increase with a decrease in sphericity.
- The top-of-bed *liquid distribution* drastically influences the flow pattern (Ravindra et al., 1997b), but a drip-point-density exceeding 5000 points per m^2 is sufficient to negate the initial maldistribution (Burghardt et al., 1995).
- The liquid-solid *contact angle* affects the way that the liquid spreads over the solid and therefore impacts the hydrodynamics indirectly. In general, porous particles are considered to have contact angles close to zero (Ravindra et al., 1997b).

- The trickle-to-pulse flow *regime transition* shifts to higher gas and liquid velocities when the pressure (or gas density), particle diameter, porosity or surface tension is increased and to lower velocities for higher liquid density. The fluid viscosity has little effect in the typical ranges (Larachi et al., 1999, Al-Dahhan et al., 1997). Enlarging the trickle flow regime makes hydrodynamic multiplicity more important.
- There is no indication that the operating *temperature* has any influence on the hydrodynamics apart from changing the fluid properties and possible liquid vaporization effects (Dudukovic et al., 2002).

In addition to the trends mentioned so far, the hydrodynamic parameters themselves are obviously inter-connected. For example, a higher wetting efficiency is obviously associated with increased liquid-solid mass transfer area and therefore a higher volumetric mass transfer coefficient. However, this assumes that whatever mechanism that was responsible for the increased wetting has not also influenced k_{LS} as well (which is unlikely in general). A cause-effect diagram (as used by Kundu et al., 2003) is misleading. For example, wetting efficiency increases with increasing holdup. Now, it is true that increased holdup results in better spreading and therefore higher wetting efficiency. It is also true that higher wetting corresponds to increased liquid-solid drag force area which in turn results in increased holdup. Wetting and holdup therefore have a symbiotic relationship that is more complex than a cause-effect diagram can indicate. There are many such complexities involved here and they are the motivation behind presenting Table 4 without the inter-connections between the hydrodynamic parameters themselves.

This concludes a brief overview of trickle flow hydrodynamics that serves as the background for an investigation into hydrodynamic multiplicity. The trends reported in this section will be re-examined (and to a fair degree explained) in connection with the hydrodynamic models of section 2.3.

2.2 Experimental Investigations into Multiplicity

Hydrodynamic multiplicity was first noticed by Kan & Greenfield (1978) and has since enjoyed ample attention from various researchers. This section presents the data of all previous experimental studies that incorporate hydrodynamic multiplicity in the broadest sense of the word. This excludes the well-known but unrelated phenomenon of temperature induced hysteresis that is due to the thermal capacity of the solid in a non-isothermal reaction (Watson & Harold, 1993). Recall that the term hydrodynamic multiplicity is taken to include both hysteresis loops and the effects of pre-wetting. It is first important to explore the relationships between hysteresis loops, pre-wetting procedures and periodic operation.

2.2.1 Hysteresis and Pre-wetting

There are two major concepts involved in previous experimental studies: hysteresis loops and pre-wetting procedures. Hysteresis loops involve increasing and then decreasing some operating variable (like liquid flow rate) during operation, whereas pre-wetting refers to some procedure (like flooding and/or draining) that is applied to the bed before operation commences. Hysteresis loops were the first manifestations of hydrodynamic multiplicity and judging from recent literature it remains the preferred way of thinking about hydrodynamic multiplicity. A recent review from Maiti et al. (2006) summarizes the early major works on hysteresis loops. A hysteresis loop is shown schematically in Figure 4. For illustrative purposes pressure drop is shown as a function of liquid velocity. The hysteresis loop is obtained as follows:

- Starting from a low (or zero) liquid velocity, the liquid flow rate is increased incrementally. The pressure drop increases accordingly (following the blue line) and reaches points A, B and C at liquid velocities $u_{L,1}$, $u_{L,2}$ and $u_{L,pulse}$ respectively.
- Further increasing the velocity beyond the trickle-to-pulse flow boundary also increases the pressure drop (following the grey line).

- When the velocity is decreased, the pressure drop decreases along the same path (grey) until $u_{L,pulse}$ is reached. Further decreasing u_L sees the pressure drop decreasing along the black line (which may be several times higher than the corresponding values on the increasing blue leg). At $u_{L,1}$ the pressure drop reaches point D. Note that all the operating conditions at this point are identical to those at point A – the only difference between the upper and lower legs is the history of the flow rate.

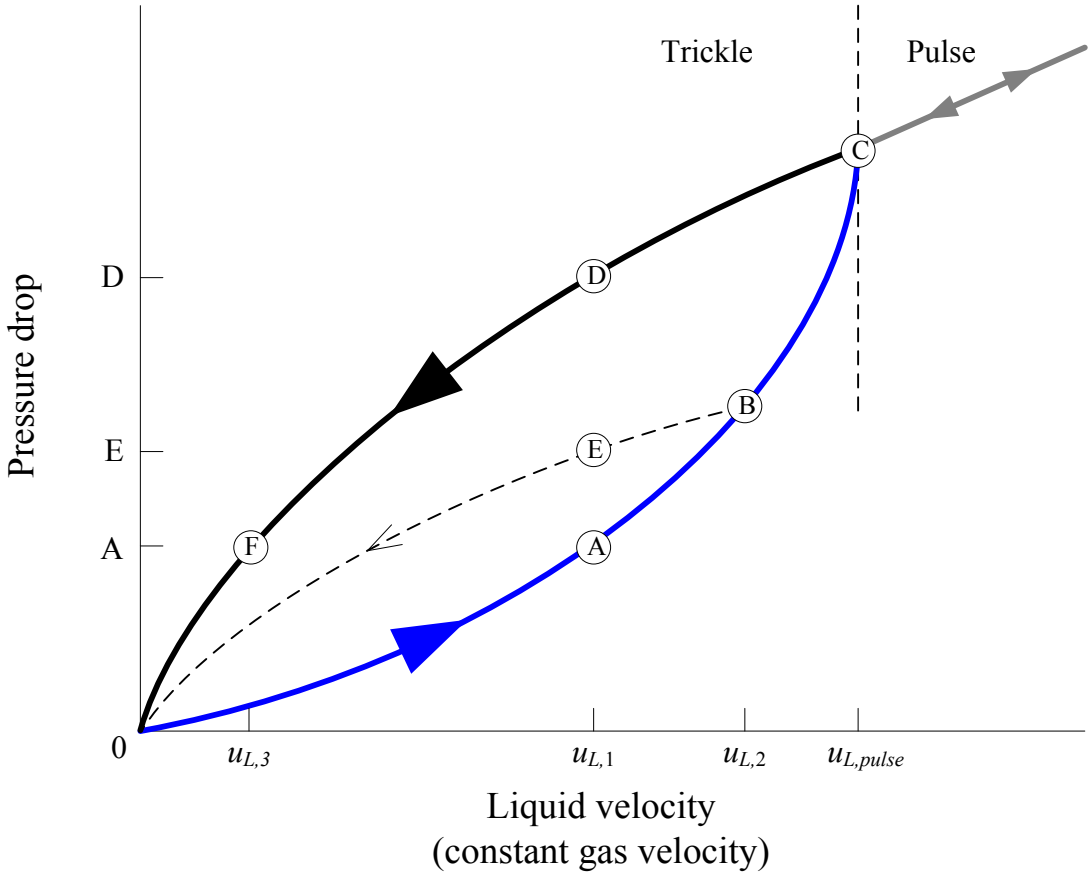

Figure 4. A schematic hysteresis loop (based on Levec et al., 1986)

Interestingly, when the liquid velocity is increased from zero to $u_{L,2}$ (which is smaller than $u_{L,pulse}$) and then decreased, the pressure drop follows the dashed line and reaches point E at $u_{L,1}$. This means that at $u_{L,1}$, any pressure drop between that of points A and D can be attained. It is important to note that all of these observations are at steady state, i.e.

when the flow rate is increased from zero to $u_{L,1}$, the pressure drop stabilizes at point A and when the flow rate is decreased from $u_{L,pulse}$ to $u_{L,1}$, pressure drop stabilizes at point D. Figure 4 depicts a *liquid flow rate variation induced hysteresis loop* because the liquid flow rate was manipulated in order to achieve a change in the hydrodynamic state. There can also be *gas flow rate variation induced hysteresis loops* (where the liquid flow rate is kept constant and the gas flow rate is manipulated to get hysteresis) or *surface tension change induced hysteresis* (where the surface tension is changed momentarily before returning it to the original value).

Hysteresis loops are not the only manifestations of hydrodynamic multiplicity. Since the hydrodynamic state of the bed depends critically on earlier conditions within the bed, it can also be altered by adopting a different pre-wetting procedure. For example, Kan & Greenfield (1978) first performed a liquid flow rate variation induced hysteresis loop (to get to point D on Figure 4) and then performed gas flow rate variation induced hysteresis. Levec et al. (1986), on the other hand, first pre-flooded and drained their bed and then performed liquid flow rate variation induced hysteresis loops. Of course, there are many combinations of pre-wetting procedures and hysteresis loops that can be performed. For example, if we have a bed pre-wetted according to the procedure in Levec et al. (1986) and once operation has been established on the upper branch of the hysteresis loop (say point D in Figure 4), the lower branch (point A) can again be reached by draining the bed and increasing the flow rate from a low value. However, if the bed had not been pre-wetted, draining the bed and re-establishing the flow will result in a pressure drop somewhere between A and D (this will be explored experimentally in Chapter 4). This can obviously become very complicated and it is necessary to define a conceptual framework by which the literature on hydrodynamic multiplicity can be interpreted. This is the first objective of this thesis and is presented next. Afterwards, all previous literature is summarized within this framework.

2.2.2 Framework of Limiting Cases

In the discussion around Figure 4, it was mentioned that the pressure drop can take any value between points A and D. Points A and D are therefore limiting cases for pressure drop variation as a result of liquid flow rate manipulation. A thorough examination of all literature indicates that there are five potential limiting cases of hydrodynamic multiplicity, as defined in Table 5. These procedures will result in one (or more) of the hydrodynamic parameters adopting a maximum (upper limit) or minimum (lower limit) value. The limiting cases are also referred to as *modes*.

Table 5. The five limiting cases (modes) of hydrodynamic multiplicity

Name	Description
Non-pre-wetted mode	Dry particles are loaded into a dry reactor. Gas and liquid flow rates are increased from zero to the operating values.
Levec pre-wetted mode	Dry particles are loaded into a dry reactor. The reactor is flooded completely for several hours and then drained under gravity until only the residual liquid holdup remains in the bed. The liquid and then the gas flow rates are increased from zero to the operating values. (It was observed that draining under gas flow at the operating velocity had a negligible effect on the hydrodynamic state).
Super pre-wetted mode	Dry particles are loaded into a dry reactor. The reactor is flooded completely for several hours and then drained. However, liquid is introduced at the operating velocity the moment that draining commences. Gas is introduced at the operating velocity a few moments after the liquid.
Kan-Liquid pre-wetted mode	Dry particles are loaded into a dry reactor. The reactor is flooded for several hours and then drained. The gas flow is introduced at the operating velocity. Keeping the gas flow rate constant, the liquid flow rate is increased from zero to a value greater than the pulsing velocity and the pulsing regime is maintained for several seconds. The liquid flow rate is then reduced to the operating value.
Kan-Gas pre-wetted mode	Dry particles are loaded into a dry reactor. The reactor is flooded for several hours and then drained. The liquid flow is introduced at the operating velocity. Keeping the liquid flow rate constant, the gas flow rate is increased from zero to a value greater than the pulsing (or spray flow) velocity and the pulsing (or spray) regime is maintained for several seconds. The gas flow rate is then reduced to the operating value.

The importance of this framework is in the fact that it makes it possible to identify categorical differences between the results of different investigators (as will be seen later in this chapter). Also, it suggests that the *extent* of hydrodynamic multiplicity and the major *trends* by which multiplicity manifests itself can be studied experimentally by looking at these five modes. Note that the identification of a conceptual framework is one of the major steps in the strategy outlined in Figure 1.

A few other pre-wetting procedures may be possible. For example, loading the particles into a flooded bed or operating in a liquid up-flow fluidized mode before establishing gas-liquid trickle flow at the operating rates. There is no indication that these procedures will influence the hydrodynamics apart from changing the bed structure and they are of little practical significance.

2.2.3 Holdup and Pressure Drop

Holdup and pressure drop are the two most studied hydrodynamic parameters in literature (Dudukovic et al., 2002). This is because a high value for holdup is generally associated with a large gas-liquid interfacial area and high liquid-solid wetting efficiency (i.e. large liquid-solid area and high particle effectiveness factors). A high pressure drop indicates a high degree of gas-liquid interaction and pressure drop is roughly indicative of the operating cost of the reactor (Kan & Greenfield, 1978).

The behaviour of holdup and pressure drop with gas and liquid flow rate variation in each of the modes is shown qualitatively in Figure 5. It represents an amalgam of the data of the references listed in the figure. The extent has been defined as the area between the upper and lower branches of the pressure drop hysteresis loop obtained by variation of the gas or liquid velocities (Maiti et al., 2005). Such numbers (in units of $\frac{kPa}{m}\frac{m}{s}$) are appropriate when the effects of different operating or system conditions on hysteresis is being examined (Maiti et al., 2006), but do not give us an intuitive feel for the extent and

applies only to pressure drop hysteresis. A simpler measure that most authors report, is the increase (at the same conditions) that is achieved in the value of the hydrodynamic parameter (e.g. pressure drop) when the operating variable (e.g. liquid velocity) is manipulated to its maximum extent. This then is the same as moving from one multiplicity mode to another as shown in Figure 4. **Error! Not a valid bookmark self-reference.** reports such values and is intended to provide a rough indication of how sensitive pressure drop and holdup is to hydrodynamic multiplicity, i.e.:

$$\text{Hysteresis Extent} = \frac{[\text{Value on upper branch}]}{[\text{Value on lower branch}]} \qquad (1)$$

These should be interpreted as the follows: for changes in gas velocity at constant liquid velocity starting from the Kan-Liquid mode (i.e. as shown in Figure 5q), the pressure drop can be *up to 2 times lower* after a gas velocity loop has been completed. This is equivalent to jumping from the Kan-Liquid to the Kan-Gas mode (as studied by Kan & Greenfield, 1978). From Table 6 we see that the pressure drop in the Kan-Liquid mode is up to 2 times higher the pressure drop in the Levec mode (data from Christensen et al., 1986 and Wang et al., 1995). Note also that it is easier to manipulate holdup by changing the liquid flow rate than by changing the gas flow rate. This has also been observed by Christensen et al. (1986) and Levec et al. (1988).

Note that the effect of gas velocity variation induced hysteresis is different in the Levec and Kan-Liquid modes (Figure 5m and Figure 5q). This is attributable to the major flow pattern differences between these modes (Wang et al., 1995) and will be returned to in later chapters.

Table 6 gives a rough indication of the *extent* of multiplicity in pressure drop and holdup as reported by the investigators referenced (the exact values obviously depend on other factors as well). Various definitions exist for expressing the extent of hysteresis.

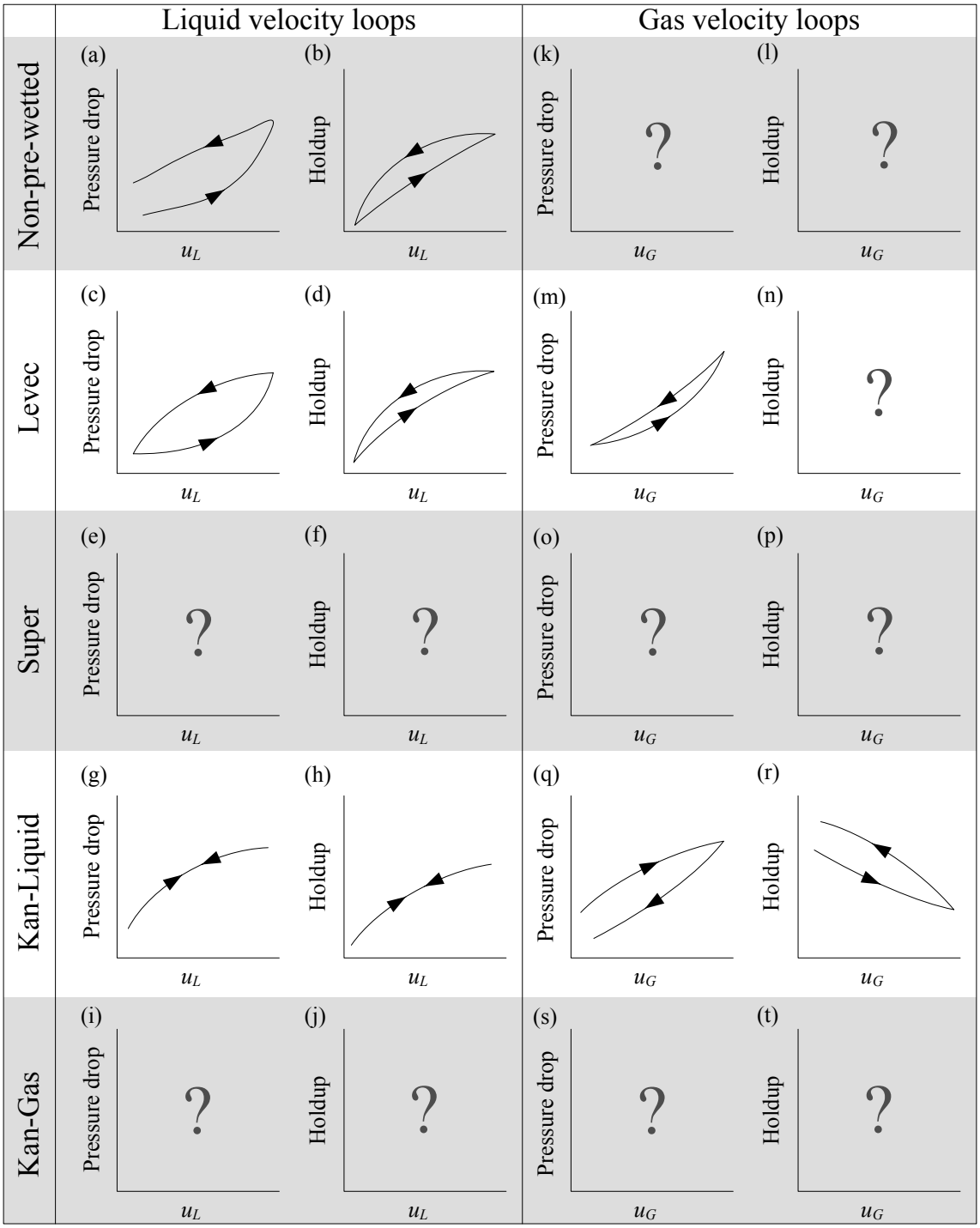

Figure 5. Single loop hysteresis for pressure drop and liquid holdup as functions of liquid (a-j) and gas (k-t) velocities (based on Kan & Greenfield, 1978, Kan & Greenfield, 1979, Levec et al., 1986, Levec et al., 1988, Christensen et al., 1986 and Wang et al., 1995)

The extent has been defined as the area between the upper and lower branches of the pressure drop hysteresis loop obtained by variation of the gas or liquid velocities (Maiti et al., 2005). Such numbers (in units of $\frac{kPa}{m}\frac{m}{s}$) are appropriate when the effects of different operating or system conditions on hysteresis is being examined (Maiti et al., 2006), but do not give us an intuitive feel for the extent and applies only to pressure drop hysteresis. A simpler measure that most authors report, is the increase (at the same conditions) that is achieved in the value of the hydrodynamic parameter (e.g. pressure drop) when the operating variable (e.g. liquid velocity) is manipulated to its maximum extent. This then is the same as moving from one multiplicity mode to another as shown in Figure 4. **Error! Not a valid bookmark self-reference.** reports such values and is intended to provide a rough indication of how sensitive pressure drop and holdup is to hydrodynamic multiplicity, i.e.:

$$\text{Hysteresis Extent} = \frac{[\text{Value on upper branch}]}{[\text{Value on lower branch}]} \qquad (1)$$

These should be interpreted as the follows: for changes in gas velocity at constant liquid velocity starting from the Kan-Liquid mode (i.e. as shown in Figure 5q), the pressure drop can be *up to 2 times lower* after a gas velocity loop has been completed. This is equivalent to jumping from the Kan-Liquid to the Kan-Gas mode (as studied by Kan & Greenfield, 1978). From **Error! Not a valid bookmark self-reference.** we see that the pressure drop in the Kan-Liquid mode is up to 2 times higher the pressure drop in the Levec mode (data from Christensen et al., 1986 and Wang et al., 1995). Note also that it is easier to manipulate holdup by changing the liquid flow rate than by changing the gas flow rate. This has also been observed by Christensen et al. (1986) and Levec et al. (1988).

Note that the effect of gas velocity variation induced hysteresis is different in the Levec and Kan-Liquid modes (Figure 5m and Figure 5q). This is attributable to the major flow

pattern differences between these modes (Wang et al., 1995) and will be returned to in later chapters.

Table 6. Typical differences in pressure drop and holdup due to multiplicity

Modes changed from:	**Illustration**	**Manipulated variable:**	**Extent: Pressure drop**	**Extent: Holdup**
Non-pre-wetted to Super	Figure 5(a-b)	*pre-flooding*	< 3.5	?
Levec to Kan-Liquid	Figure 5(c-d)	u_L	< 2	< 1.4
Levec to Kan-Gas	Figure 5(m)	u_G	< 1.5	?
Kan-Liquid to Kan-Gas	Figure 5(q-r)	u_G	> -2	< 1.1

Data from: Kan & Greenfield (1978), Kan & Greenfield (1979), Levec et al. (1986), Levec et al. (1988), Christensen et al. (1986), Lazzaroni et al. (1989), Ravindra et al. (1997), Wang et al. (1995). **Note:** These data were not generated on the same systems – an issue addressed in Chapter 4.

Other operating variables affect hydrodynamic multiplicity in pressure drop and holdup as listed below. Although these operating variables likely influence the other hydrodynamic parameters as well, no experimental data have been reported.

- *Particle size* – Several authors (Kan & Greenfield, 1978, Levec et al., 1986, Wang et al., 1995, Ravindra et al., 1997b, Gunjal et al., 2005) have shown that an increase in particle size (with little change in porosity) reduces the extent of hysteresis. This is one trend that has not been explained satisfactorily to date (and will be returned to in Chapter 7).
- *Liquid properties* – The major factor is surface tension and has been studied by several authors (see Table 7). Lutran et al. (1991) reports that lowering the surface tension in a Non-pre-wetted bed has the effect of preserving filament/rivulet flow but the rivulets meander less. In the Super mode, lower surface tension resulted in more filament-type flow, although it is unclear what constitutes a filament. In more quantitative terms, Kan & Greenfield (1978), Christensen et al. (1986) and Wang et al. (1995) report that lowering the surface tension increases the pressure

drop but had little effect on the extent of pressure drop hysteresis, while Levec et al. (1986) showed that holdup hysteresis is less pronounced at lower surface tension values.

- *Gas properties* (pressure) – The effect of pressure (or gas density) on the extent of hydrodynamic multiplicity has not been addressed. The general expectation is that increased gas density would result in less hysteresis. This is based on the argument that increased gas density results in increased gas-liquid shear that helps to distribute the liquid (Al-Dahhan & Dudukovic, 1995). Uniform liquid distribution in the bed is in turn associated with less hysteresis (Wang et al., 1995). This is yet to be validated or refuted by experiment (see Chapter 4).
- Levec et al. (1986) investigated the difference in holdup and pressure drop between the Levec and Super modes as *gas velocity* is increased. The results for holdup are shown in Figure 6. Apart from reducing the trickle-to-pulse flow transition liquid velocity, higher gas velocities do not alter the extent of hysteresis except at very high gas velocity.

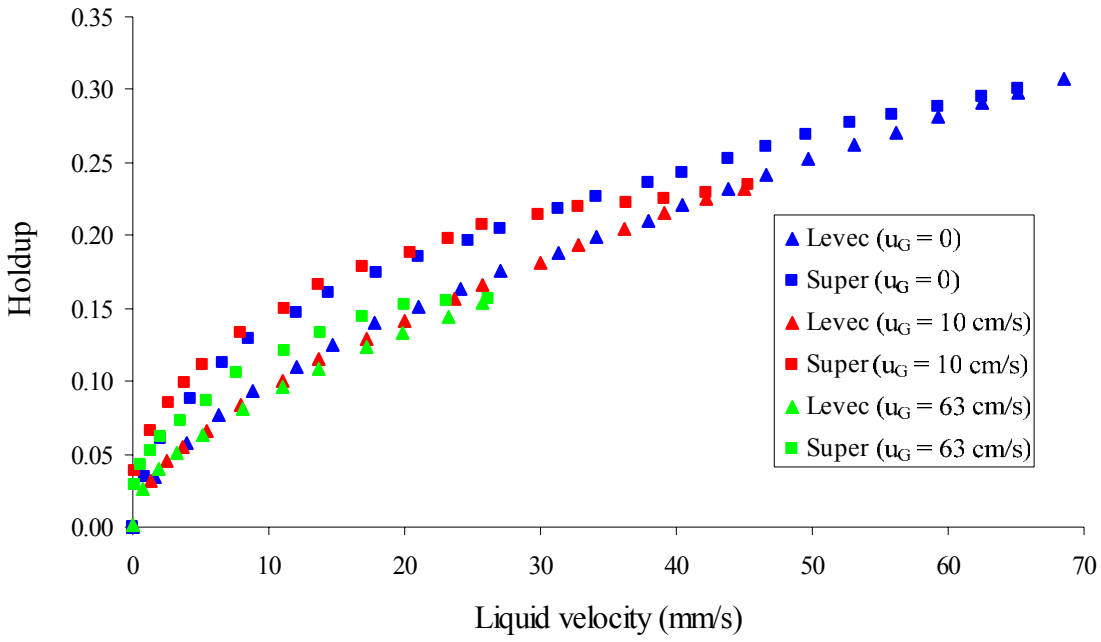

Figure 6. Effect of gas velocity on the difference between Levec and Super modes (data from Levec et al., 1986)

One major drawback in all of these analyses is the fact that none of the authors investigated all the multiplicity modes for their chosen systems. Quantitative comparisons are therefore very difficult to make. See section 4.1 for such quantitative comparisons in all the modes for a single system.

2.2.4 Mass Transfer Coefficients

The volumetric gas-liquid mass transfer coefficient also exhibits multiple hydrodynamic states, as shown by physical desorption/absorption methods. Wammes et al. (1991) reported that the gas-liquid mass transfer area in the Kan-Liquid mode is higher than that in the Levec mode. Wang et al. (1994) and Wang et al. (1997) showed that the volumetric gas-liquid mass transfer coefficient in the Kan-Liquid mode is up to 2.3 times higher than in the Levec mode, while it is up to 1.45 times higher in the Kan-Gas mode than in the

Levec mode. They found that gas velocity variation induced hysteresis starting from the Kan-Liquid mode (i.e. going from Kan-Liquid to Kan-Gas) had little effect on the transfer coefficient. Single loop hysteresis trends are illustrated in Figure 7.

Only one study has reported hydrodynamic multiplicity for the liquid-solid volumetric mass transfer coefficient. Sims et al. (1993) measured averaged particle scale liquid-solid mass transfer coefficients using an electrochemical technique with solid and hollow cylinders. They first established steady flow in the Kan-Liquid mode (i.e. pulse pre-wetting) and then performed liquid flow rate variation induced hysteresis loops. They found that the coefficient on the decreasing leg was up to roughly 1.5 times higher than on the increasing leg (see Figure 7h for a schematic diagram). Note that a similar procedure results in *no hysteresis* of either pressure drop or holdup (refer back to Figure 5).

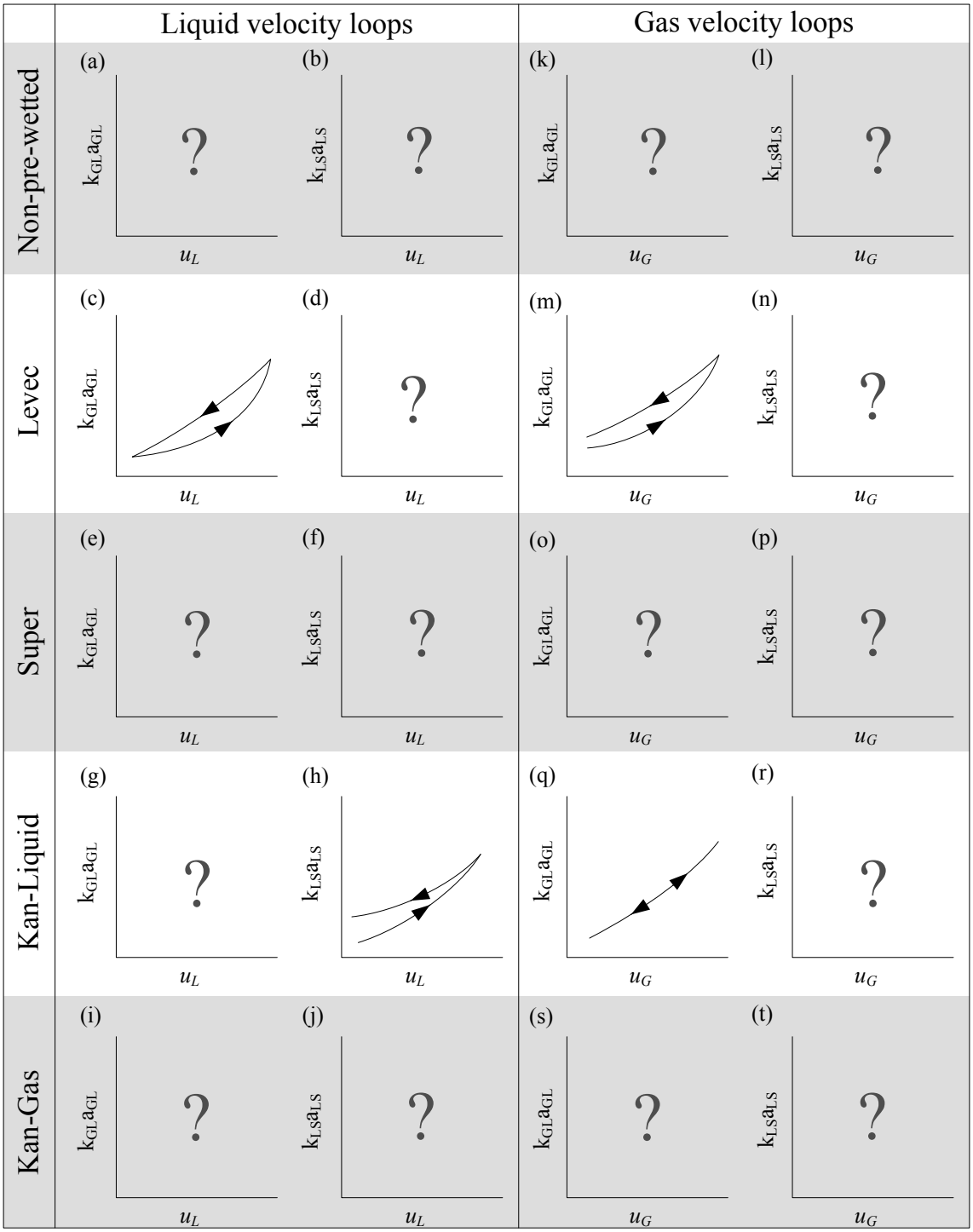

Figure 7. Single loop hysteresis for mass transfer coefficients as functions of liquid (a-j) and gas (k-t) velocities (based on Wammes et al., 1991, Wang et al., 1994, Wang et al., 1997 and Sims et al., 1993)

2.2.5 Wetting Efficiency

Since wetting efficiency impacts the gas-solid and liquid-solid mass transfer areas as well as the particle effectiveness (through the internal diffusion boundary conditions), it is of paramount importance in trickle bed reactor design. This is particularly true for low liquid velocities where hydrodynamic multiplicity can be expected to play a major role. Using colorimetric methods, Lazzaroni et al. (1988 and 1989) showed that the Super mode has larger wetting efficiencies than the Non-pre-wetted mode (up to 3 times higher). They also showed how the wetting is maldistributed over the bed cross-section. Starting from the Super mode, an increase in gas velocity decreased the wetting efficiency (contrary to the results of Al-Dahhan & Dudukovic (1995) who used tracer methods). Ravindra et al. (1997b) later confirmed these results (also using a colorimetric method and different particle sizes and distributors).

Most recently, Van Houwelingen et al. (2006) showed a 16-25% increase in wetting efficiency in going from the Levec to the Kan-Liquid modes and found that gas velocity increases had little effect on the wetting efficiency and the particle wetting distributions. Sederman & Gladden (2001) used magnetic resonance imaging to determine the wetting efficiency and found that the Levec mode had 2.9-3.6 times higher wetting than the Non-pre-wetted mode, and that the Kan-Liquid mode had twice the wetting efficiency of the Levec mode.

2.2.6 Liquid Distribution

The distribution of the liquid over the cross-section has been linked to all of the observed trends mentioned thus far. Originally, Christensen et al. (1986) identified two types of flow: film flow and rivulet or filament flow. Although difficult to quantify, the existence of multiple flow morphologies have been confirmed through other techniques. After extensive experimental work, Wang et al. (1999) concluded that the hydrodynamic multiplicity trends observed in pressure drop, holdup and axial dispersion can be

attributed to hysteresis of the liquid distribution. However, this issue has not received adequate attention in literature (Kundu et al., 2001). It is therefore necessary to review this topic in greater detail.

Liquid maldistribution (M) is usually quantified as the second moment of the distribution of some hydrodynamic parameter (x) around its mean (x_{mean}):

$$M = \sqrt{\frac{1}{N(N-1)}\sum_i \left(\frac{x_i - x_{mean}}{x_{mean}}\right)^2} \qquad (2)$$

Here x can be any of the hydrodynamic parameters listed in Table 2 or it is often taken as the volumetric flow rate of liquid (or gas) through an annular collector cell (Ravindra et al., 1997b, Wang et al., 1998c). An example is given in Figure 8(a). It is imperative to note that the values of M calculated from such data depend critically on how the cross-sectional area is divided (i.e. the area of each cell). Values of M are therefore only meaningful for a specific collector design. When tomography is used, holdup is often chosen as x (see Figure 8(b), Marcandelli et al., 2000). Other approaches have also been followed. Christensen et al. (1986) defined the fraction film flow as the ratio of the velocities in the Kan-Liquid and Levec modes for the same pressure drop (i.e. in Figure 4 the fraction film flow at a pressure drop of A is equal to $u_{L,3}$ divided by $u_{L,1}$), and showed that this fraction increases with liquid velocity (implying that the Levec mode tends more and more to the Kan-Liquid mode as velocity is increased, see Figure 8f). Liquid distribution is generally better at higher liquid velocity (Marcandelli et al., 2000). Lazzaroni et al. (1988) measured wetting in three concentric zones and showed that these follow the local liquid flow rates in these zones. This data was later extended to include other system conditions (non-porous packing and different distributor types) by Ravindra et al. (1997b). Wang et al. (1997) showed how the local liquid flow rate and gas-liquid mass transfer coefficient distributions are related. Later, Wang et al. (1999) showed that pressure drop hysteresis and liquid flux distribution hysteresis are also correlated (the better the liquid flux distribution the higher the pressure drop).

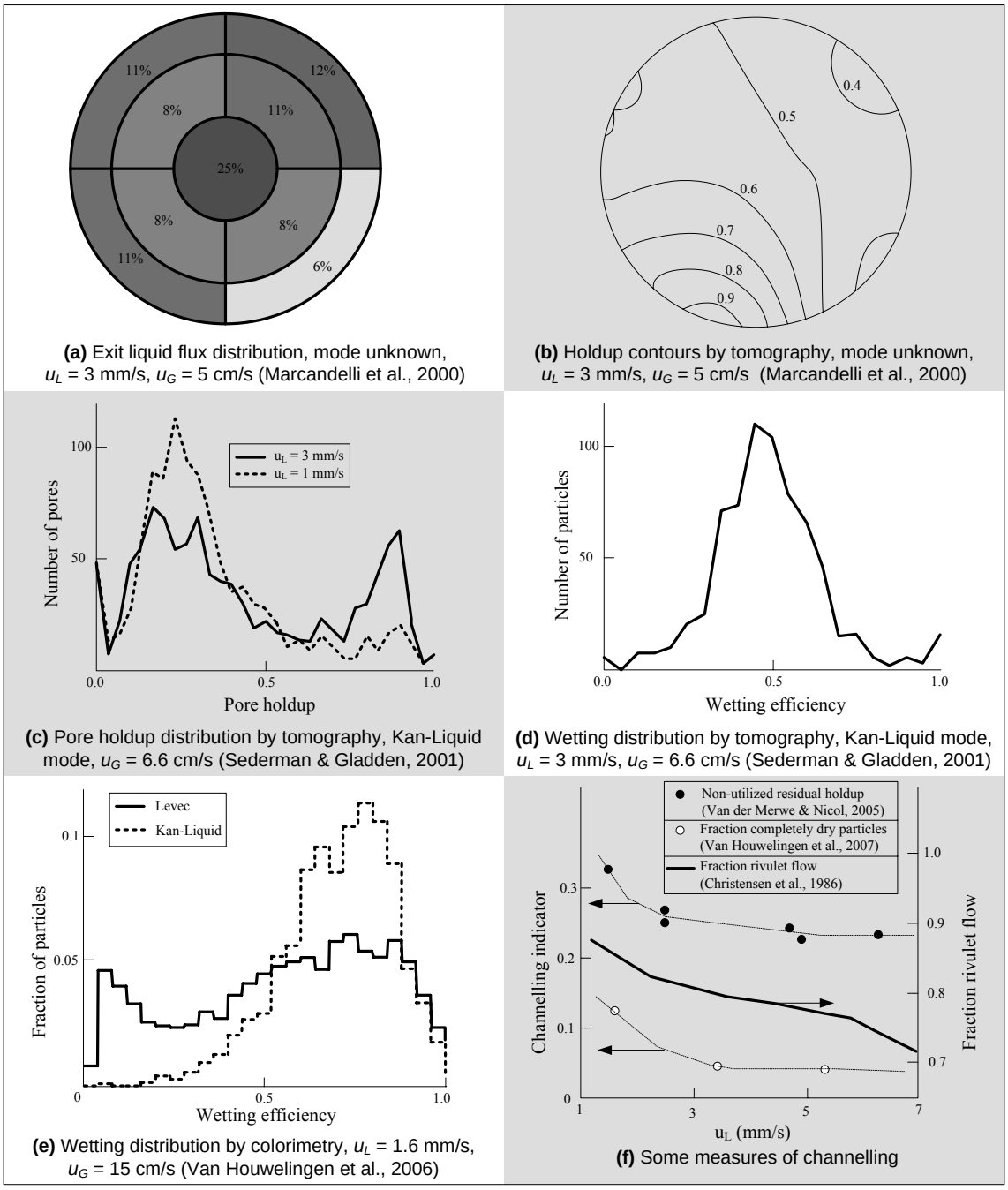

(a) Exit liquid flux distribution, mode unknown, u_L = 3 mm/s, u_G = 5 cm/s (Marcandelli et al., 2000)

(b) Holdup contours by tomography, mode unknown, u_L = 3 mm/s, u_G = 5 cm/s (Marcandelli et al., 2000)

(c) Pore holdup distribution by tomography, Kan-Liquid mode, u_G = 6.6 cm/s (Sederman & Gladden, 2001)

(d) Wetting distribution by tomography, Kan-Liquid mode, u_L = 3 mm/s, u_G = 6.6 cm/s (Sederman & Gladden, 2001)

(e) Wetting distribution by colorimetry, u_L = 1.6 mm/s, u_G = 15 cm/s (Van Houwelingen et al., 2006)

(f) Some measures of channelling

Figure 8. Recent liquid distribution results. (a) Annular collector liquid flux results, (b) Capacitance tomography holdup contours, (c) Pore holdup distribution for two velocities by tomography, (d) A particle wetting distribution (PWD) by tomography, (e) PWDs by colorimetry showing uni-modal and bi-modal character in Kan-Liquid and Levec modes respectively, (f) Levec mode channelling.

Sederman & Gladden (2001) obtained tomographical images of the Non-pre-wetted, Levec and Kan-Liquid modes. They further partitioned the void space into pores and calculated pore holdup distributions (Figure 8c) as well as particle wetting distributions (Figure 8d). They found a bi-modal holdup distribution at higher velocities and took this to be indicative of the actual flow pattern adopting some mixture of film flow and rivulet flow. Basavaraj et al. (2005) used radiographical imaging in a two dimensional bed with non-pre-wetted packing and showed that the holdup is not uniformly distributed throughout the bed even after the liquid flow rate was increased (up to 1 mm/s from 0.2 mm/s) and decreased. In an earlier study (Van der Merwe & Nicol, 2005), the author of this thesis investigated the liquid distribution of the Non-pre-wetted, Levec and Super modes for zero gas flow (Figure 8f). The distribution was quantified in terms of the utilization of the residual liquid holdup. It was found that this utilization coefficient is higher in the Levec mode (values of 0.40-0.85) than in the Non-pre-wetted mode (0.2-0.8) and even higher (close to unity) in the Super mode. The utilization was incorporated into a hysteresis model capable of predicting holdup in each of the modes. Van Houwelingen et al. (2006) used a colorimetric technique to get particle wetting distributions in the Levec and Kan-Liquid modes (Figure 8e). They showed that in the Levec mode particles are either well wetted or very poorly wetted (bi-modal distribution) and took this to indicate rivulet flow. In the Super mode, all the particles were approximately wetted at the bed average, indicating film flow. Recently, Van Houwelingen et al. (2007) have suggested that the best measure of channelling is the fraction of particles that are completely non-wetted, i.e. $f = 0$.

It is imperative to note that these trends are aggravated when point or line distributors are used, but that a perfectly uniform distribution does not change the fact that different flow patterns persist in the different modes (Lutran et al., 1991). Figure 8 shows some of the results of the more recent investigations.

While it is clear that the liquid distribution is central to the understanding of hydrodynamic multiplicity (Wang et al., 1999), it remains unclear why the liquid

distributes itself in these ways and section 2.3 reviews some proposed mechanisms. Resolving this issue is one of the main objectives of this thesis.

2.2.7 Summary of Experimental Studies

Table 7 presents an exhaustive list of all published literature (to date) that investigated some aspect of hydrodynamic multiplicity *experimentally*. It is presented in chronological order. The major findings of these studies have already been summarized in the preceding sections and are not repeated here. Papers based on work in the present thesis have not been included.

Table 7. Summary of experimental studies of hydrodynamic multiplicity

Reference	System properties						Hydrodynamics investigated							Modes investigated				
	u_L (mm/s)	u_G (cm/s)	σ (mN/m)	d (mm)	Porous/ Non-porous	Dist.*	ε_L	$\Delta P/\Delta z$ (kPa/m)	$k_{GL}a_{GL}$ (1/s)	$k_{LS}a_{LS}$ (1/s)	f	D_{AX} (m^2/s)	M	NP	L	S	KL	KG
Kan & Greenfield (1978)	1-10	2-100	38, 70	0.5, 1, 1.8	Non-porous	U	**Y**	**Y**	**N**	**N**	**N**	**N**	**N**	**N**	**N**	**N**	**Y**	**Y**
Levec et al. (1986)	0.1-25	0-40	39-73	3, 6	Non-porous	U	**Y**	**Y**	**N**	**N**	**N**	**N**	**N**	**N**	**Y**	**Y♠**	**Y**	**N**
Christensen et al. (1986)	0-11	0-55	<70, 70	3	Non-porous	U, L	**Y**	**Y**	**N**	**N**	**N**	**N**	**Y**	**N**	**Y**	**N**	**Y**	**Y**
Levec et al. (1988)	0-20	0-21	70	3	Non-porous	U	**Y**	**Y**	**N**	**N**	**N**	**N**	**N**	**N**	**Y**	**Y♠**	**Y**	**Y**
Lazzaroni et al. (1988)	2-6	0-8	≈70	≈3	Porous	U	**N**	**N**	**N**	**N**	**Y**	**N**	**Y**	**Y**	**N**	**Y**	**N**	**N**
Lazzaroni et al. (1989)	0.8-8.4	2-8	≈70	3	Porous	U, P	**Y**	**Y**	**N**	**N**	**Y**	**N**	**N**	**Y**	**N**	**Y**	**N**	**N**
Lutran et al. (1991)	3, 6, 9	0	28-72	3, 6	Non-porous	U, L, P	**N**	**N**	**N**	**N**	**N**	**N**	**Y♣**	**Y♠**	**N♥**	**Y♠**	**N**	**N**
Wammes et al. (1991)	3-12	1, 2.5	?	3	Non-porous	U	**N**	**Y**	**Y**	**N**	**N**	**N**	**N**	**N**	**Y**	**N**	**Y**	**N**
Sims et al. (1993)	1-6	14	≈70	2 x 3	Non-porous	U	**N**	**N**	**N**	**Y**	**N**	**N**	**N**	**N**	**N**	**N**	**Y**	**N**

Y = Yes, **N** = No, * Distributor options: P = Point, L = Line, U = Uniform, Modes: NP = Non-pre-wetted, L = Levec, S = Super, KL = Kan-Liquid, KG = Kan-Gas.
♠ Only with no gas flow, ♣ Only qualitatively, ♥ Authors erroneously grouped Levec and Super modes together.

Table 7. Summary of experimental studies of hydrodynamic multiplicity (continued)

Reference	System properties						Hydrodynamics investigated							Modes investigated				
	u_L (mm/s)	u_G (cm/s)	σ (mN/m)	d (mm)	Porous/ Non-porous	Dist.*	ε_L	$\Delta P/\Delta z$ (kPa/m)	$k_{GL}a_{GL}$ (1/s)	$k_{LS}a_{LS}$ (1/s)	f	D_{AX} (m^2/s)	M	NP	L	S	KL	KG
Wang et al. (1994)	0-15	5-55	70	2.7, 4	Non-porous	?	**N**	**N**	**Y**	**N**	**N**	**N**	**N**	**N**	**Y**	**N**	**Y**	**Y**
Wang et al. (1995)	0-22	5-55	57, 73	2.7, 4, 8	Non-porous	U	**N**	**Y**	**N**	**N**	**N**	**N**	**N**	**N**	**Y**	**N**	**Y**	**Y**
Wang et al. (1997)	0-15	20.8	73	2.7	Non-porous	U	**N**	**N**	**Y**	**N**	**N**	**N**	**Y**	**N**	**Y**	**N**	**Y**	**N**
Ravindra et al. (1997a)‡	1-7	1.7	≈70	1.9	Porous	U	**N**	**N**	**N**	**N**	**N**	**N**	**N**	**Y**	**N**	**Y**	**N**	**N**
Ravindra et al. (1997b)	1-8	5	≈70	1.6/1.9, 3.5, 5.5/6.3	Both	U, L, P	**N**	**Y**	**N**	**N**	**Y♦**	**N**	**Y**	**Y**	**N**	**Y**	**N**	**N**
Rajashekharam et al. (1998) ‡	0.01-0.5	0.2-0.6	?	1, 2	Porous	P	**N**	**N**	**N**	**N**	**N**	**N**	**N**	**Y**	**N**	**N**	**N**	**N**
Wang et al. (1998)	0-17	0-23	≈70	3	Non-porous	U	**N**	**Y**	**N**	**N**	**N**	**N**	**Y**	**N**	**Y**	**N**	**Y**	**Y**
Wang et al. (1999)	0-13	0-23	≈70	3	Non-porous	U	**N**	**Y**	**N**	**N**	**N**	**Y♪**	**Y**	**Y**	**Y**	**N**	**Y**	**N**
Jiang (2000)	0.7-11	?	≈70	3	Non-porous	U, P	**N**	**N**	**N**	**N**	**N**	**N**	**Y**	**Y**	**Y**	**N**	**N**	**N**

Y = Yes, **N** = No, * Distributor options: P = Point, L = Line, U = Uniform, Modes: NP = Non-pre-wetted, L = Levec, S = Super, KL = Kan-Liquid, KG = Kan-Gas.
‡ Reaction study (see Chapter 8), ♦ Only qualitatively, ♪ Reduced second moments of RTD outputs reported.

Table 7. Summary of experimental studies of hydrodynamic multiplicity (continued)

Reference	System properties						Hydrodynamics investigated							Modes investigated				
	u_L (mm/s)	u_G (cm/s)	σ (mN/m)	d (mm)	Porous/ Non-porous	Dist.*	ε_L	$\Delta P/\Delta z$ (kPa/m)	$k_{GL}a_{GL}$ (1/s)	$k_{LS}a_{LS}$ (1/s)	f	D_{AX} (m^2/s)	M	NP	L	S	KL	KG
Sederman & Gladden (2001)	0.5-5.8	6.6-36	≈70	5	Non-porous	U	**Y**	**N**	**N**	**N**	**Y**	**N**	**Y†**	**Y**	**Y**	**N**	**Y**	**N**
Tsochatzidis et al. (2002)	1-20	14	≈70	3.2	Porous	U, HB♫	**N**	**Y**	**N**	**N**	**N**	**N**	**N**	**Y**	**N**	**N**	**Y**	**N**
Basavaraj et al. (2005)	0.2-1	0	?	3.8	Non-porous	L	**Y**	**N**	**N**	**N**	**N**	**N**	**Y**	**Y**	**N**	**N**	**N**	**N**
Gunjal et al. (2005)	0-10	11-44	70	3, 6	Non-porous	U‡‡	**Y**	**Y**	**N**	**N**	**N**	**N**	**N+**	**Y**	**N**	**N**	**Y**	**N**
Van der Merwe & Nicol (2005)	0-17	0	70	3	Non-porous	U	**Y**	**N**	**N**	**N**	**N**	**N**	**Y**	**Y**	**Y**	**Y**	**N**	**N**
Van Houwelingen et al. (2006)	1.6, 5.4	2, 15	≈70	2.5	Porous	U	**Y**	**Y**	**N**	**N**	**Y**	**N**	**Y§**	**N**	**Y**	**N**	**Y**	**N**

Y = Yes, **N** = No, * Distributor options: P = Point, L = Line, U = Uniform, Modes: NP = Non-pre-wetted, L = Levec, S = Super, KL = Kan-Liquid, KG = Kan-Gas.
♫ HB = Half-blocked, ‡‡ Spray and plate distributors used, + Wall pressure fluctuations measured, **§** Distribution inferred from particle wetting distribution, † Pore-scale holdup distribution.

2.3 Hydrodynamic Modelling

2.3.1 Hydrodynamic Modelling in General

There are three broad approaches to correlating or modelling trickle flow hydrodynamics (Dudukovic et al., 2002):

- *Empirical methods:* The relevant hydrodynamic parameters are correlated to dimensionless groups identified by dimensional analysis. These include well-known dimensionless numbers like the Reynolds, Froude, Weber, Lockhart-Matinelli, Eötvos (Bond) and Schmidt numbers. Each number represents the ratio of two forces, namely (Iliuta et al., 1999b) the inertial-to-viscous, inertial-to-gravity, inertia-to-capillary, gas-to-liquid inertia and gravity-to-capillary forces (the Schmidt number being the momentum-diffusivity-to-mass-diffusivity ratio). The physical basis for this type of correlation is that the liquid in the bed experiences the following forces (Fukutake & Rajakumar, 1982): gravitational, inertial, viscous, surface, solid-liquid interfacial and gas-liquid interfacial forces. A correlation usually takes a power-law form. For example, Specchia & Baldi (1977) found that holdup is roughly proportional to $Re_L^{0.55}$. Other commonly used empirical correlations are those of Turpin & Huntington (1967), Ellman et al. (1988), Ellman et al. (1990) and Larachi et al. (1991). However, the pinnacle of empirical correlations is the artificial neural networks (ANN) of the group at Laval University (Larachi et al., 1999, Iliuta et al., 1999a, Iliuta et al., 1999b) that rely on a large database of experimental values. Incidentally, the ANN approach has not been applied to hydrodynamic multiplicity. This thesis aims toward addressing hydrodynamics more fundamentally and the empirical approach is not pursued.
- *Fundamental simulation:* With the advent of increased processing power, several authors have attempted to solve volume-averaged versions of the Navier-Stokes

equations of fluid flow. This computational fluid dynamic (CFD) approach is potentially the most fundamentally sound and rigorous, but suffers from what is generally described to as the closure problem. This refers to the fact that the fluid-fluid and fluid-solid boundaries need closure relations that can at present only be specified empirically (Dudukovic et al., 2002) in order to properly deal with phase interaction and issues like turbulence. Another problem with CFD is the complexity of the pore space in a packed bed. This has led to the use of an ensemble of "representative cells" where each cell encapsulates several particles and is assigned a uniform porosity (see for example Gunjal et al., 2005). It is unclear at this stage how such a cell is to be defined and how its definition impacts the calculated result. CFD is therefore not yet free from some empiricism, but even so exhibits great potential in reactor scale simulation (Kuipers & Van Swaaij, 1997).

- *Phenomenological approaches:* In the phenomenological approach, hydrodynamics are modelled by applying the laws of the conservation of mass, momentum and energy to a postulated geometry that is simple enough so that expressions for each term in these balances can be obtained. The idea has been used with great success to capture hydrodynamic trends (Dudukovic et al., 2002). Nevertheless, phenomenological models always have some adjustable parameters that need to be determined experimentally. Unfortunately, the values of these parameters do not often have sound physical meanings.

The fundamental solution and phenomenological approaches start from the general conservation law (Dudukovic et al., 2002):

(nett rate of output by phase i)
- (nett rate of input by phase i)
+ (nett rate of transport into phase i) (3)
+ (nett rate of generation in phase i)
= (rate of accumulation in phase i)

This equation is written in terms of mass, momentum and sometimes energy conservation for different geometries and on different scales. On the bed-scale and for the case of no inter-phase mass transfer and no change of phase, Iliuta & Larachi (2005) provides a generic expansion for each term, yielding:

$$\frac{\partial}{\partial t}\varepsilon_\alpha \langle \psi_\alpha \rangle^\alpha + \nabla \bullet \varepsilon_\alpha \langle \mathbf{v}_\alpha \rangle^\alpha \langle \psi_\alpha \rangle^\alpha + \nabla \bullet \langle \xi_\alpha \rangle$$
$$= \nabla \bullet \langle \Omega_\alpha \rangle + \varepsilon_\alpha \langle \sigma_\alpha \rangle^\alpha + \frac{1}{V}\iint_{A_{\alpha\beta}} \Omega_\alpha \mathbf{n} dA + \frac{1}{V}\iint_{A_{\alpha\gamma}} \Omega_\alpha \mathbf{n} dA \qquad (4)$$

Accumulation + Inertia + Dispersion
= Surface flux + Source + Transfer from β to α + Transfer from γ to α

Below equation 4, each term has been given a descriptive name. α indicates the phase (i.e. either gas or liquid) and brackets indicate α-phase volume averaged values. Although seemingly complicated, the equation simply re-states equation 3. For example, a momentum balance on the α phase is obtained by setting $\langle\psi_\alpha\rangle^\alpha$ as the momentum vector ($\rho_\alpha \boldsymbol{u}_\alpha$), $\langle\sigma_\alpha\rangle^\alpha$ as the body (gravity) force ($\rho_\alpha \boldsymbol{g}$), $\langle\Omega_\alpha\rangle^\alpha$ represents the pressure and viscous stress, and the last two terms are simply the forces exerted by the gas and solid phases on the liquid (F_{GL} and F_{SL}). Now, assuming constant phase densities, steady, uni-directional (vertical) flow and that the macroscopic inertia is negligible (i.e. the flow is fully developed in the axial direction), the momentum balance (for phase α) further reduces to (Carbonell, 2000):

$$\varepsilon_\alpha \frac{dP_\alpha}{dz} + \varepsilon_\alpha \rho_\alpha g - F_{\alpha\beta} - F_{\alpha S} \qquad \alpha = g, l \quad \text{and} \quad \beta = l, g \qquad (5)$$

Note that we have not assumed full wetting in order to obtain equation 5. It is often easier to arrive at Equation 5 by applying the overall linear momentum balance in integral form to a control volume that includes all three phases (Welty et al., 1984:49). Carbonell (2000) states that the key to obtaining any prediction is in determining the drag forces ($F_{\alpha\beta}$ and $F_{\alpha S}$). While each drag force is nearly always expressed in the Ergun (1952) formulation as the sum of a viscous and an inertial term, various approaches have been

adopted. There are six major approaches to modelling hydrodynamics. They are listed in Table 8, illustrated in Figure 9 (where possible) and discussed thereafter.

Table 8. Six major approaches to trickle flow hydrodynamic modelling

Approach	Comments	References
Relative permeability	Relatively simple. No accounting for partial wetting. Wide applicability. Low level of empiricism.	Saez & Carbonell (1985) Levec et al. (1986) Lakota et al. (2002) Nemec et al.(2001b) Fourar et al. (2001) Nemec et al. (2005a)
Slit models	Range from simple to very complicated with varying degrees of empiricism. Wide applicability. More complicated approaches account for partial wetting.	Holub et al. (1992) Holub et al. (1993) Al-Dahhan et al. (1998) Iliuta et al. (1999c) Iliuta et al. (2000) Iliuta et al. (2002) Iliuta & Larachi (2005)
Fundamental force balance	Low level of empiricism. Fully wetted flow only. Relatively simple and good applicability.	Tung & Dhir (1988) Narasimhan et al. (2002) Attou et al. (1999)
Lattice-Boltzmann simulation	Early stages of development.	Manz et al. (1999) Mantle et al. (2001) Gladden et al. (2003b)
Pore-network models	Relative high levels of empiricism and very complex. Fully wetted flow only. Little experimental validation.	Crine et al. (1979) Chu & Ng (1989) Melli & Scriven (1991)
Computational fluid dynamics	Relatively complex and computationally expensive. Boundary conditions are empirical (closure problem). Capable of dealing with 2 and 3 dimensions. Cannot yet deal with particle scale phenomena.	Jiang et al. (1999) Propp et al. (2000) Souadnia & Latifi (2001) Jiang et al. (2002) Gunjal et al. (2005)

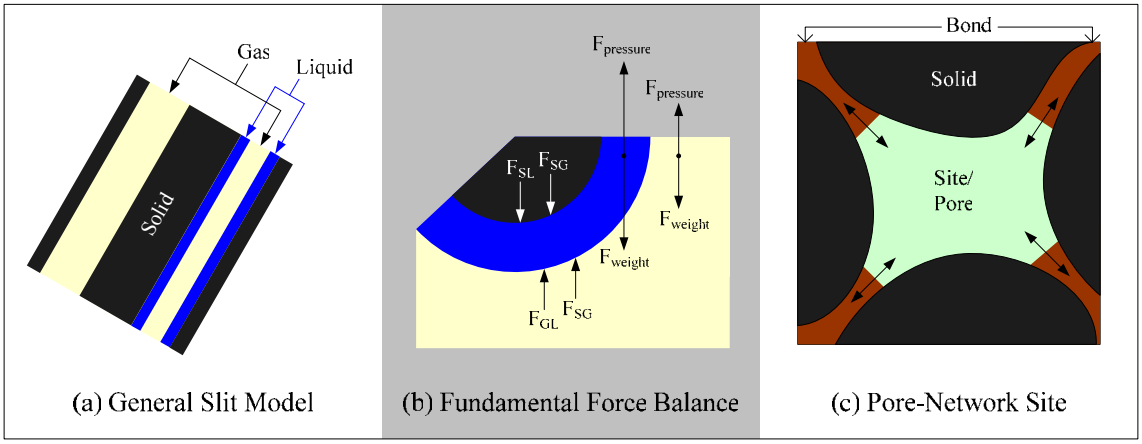

Figure 9. Geometries of three of the six modelling approaches. (a) Double slit model, (b) Fundamental forces, (c) Pore-network. See references in Table 8.

Relative Permeability Concept

The relative permeability idea starts from an Ergun-like equation for one-phase flow in a conduit (Saez & Carbonell, 1985):

$$\left(-\frac{\Delta P}{\Delta z}+\rho g\right)_{1-\text{phase}}=\frac{C_1\mu U}{D_h^2}+\frac{C_2\rho U^2}{D_h} \tag{6a}$$

The first term on the right-hand side is the Hagen-Poisseuille viscous term and the second is an inertial term derived from dimensional analysis. C_1 and C_2 are constants, U is the actual (interstitial) velocity and D_h is the hydraulic diameter (equal to 4 times the phase volume to wetted area ratio, Welty et al., 1984). The *relative* permeability concept now assumes that the two-phase flow pressure drop is equal to the one-phase flow pressure drop provided that the viscous term in equation 6 is divided by a factor k_α and the inertial term by a factor $k_{\alpha i}$:

$$\left(-\frac{\Delta P}{\Delta z}+\rho_\alpha g\right)_{2-\text{phase}}=\frac{C_1\mu_\alpha U_\alpha}{k_\alpha D_h^2}+\frac{C_2\rho_\alpha U_\alpha^2}{k_{\alpha i} D_h} \tag{6b}$$

Here α is again either gas or liquid. Usually, the viscous and inertial factors are assumed to be equal (Saez & Carbonell, 1985) and termed the relative permeability (one for each phase, i.e. k_L and k_G). They are further assumed to be functions of the phase saturations (holdups) only and correlated accordingly. Equation 6b is written for each phase (2 equations) and assuming that the pressure drop of each phase is equal to the other, these can be solved simultaneously for pressure drop and liquid holdup (2 variables). Saez & Carbonell (1985) applied this concept to the available trickle flow data and obtained best-fit expressions for the relative permeabilities in terms of the phase saturations. Similar investigations with equal success for additional low pressure data were conducted by Levec et al. (1986) and Lakota et al. (2002). Each of these studies report slight variations to the original Saez & Carbonell (1985) correlations. Recently, Nemec & Levec (2005b) generated a comprehensive set of experimental data and showed that very satisfactory predictions can be obtained for high pressure operation with a variety of systems (including differently sized spherical, cylindrical and tri-lobed particles). The most recent forms of the relative permeability equations are (Nemec & Levec, 2005b):

$$\frac{1}{k_L}\left[A\frac{\mathrm{Re}_L^*}{Ga_L^*}+B\frac{\mathrm{Re}_L^{*2}}{Ga_L^*}\right]\frac{\rho_L}{\rho_L-\rho_G}-\frac{1}{k_G}\left[A\frac{\mathrm{Re}_G^*}{Ga_G^*}+B\frac{\mathrm{Re}_G^{*2}}{Ga_G^*}\right]\frac{\rho_G}{\rho_L-\rho_G}=1 \tag{7}$$

$$-\frac{\Delta P}{\Delta z}\frac{1}{\rho_G g}=\frac{1}{k_G}\left[A\frac{\mathrm{Re}_G^*}{Ga_G^*}+B\frac{\mathrm{Re}_G^{*2}}{Ga_G^*}\right] \tag{8}$$

$$k_L=\begin{cases}\delta^{2.9} & \delta\geq 0.3\\ 0.4\delta^{2.1} & \delta<0.3\end{cases}\qquad \delta=\frac{\varepsilon_L-\varepsilon_{L,res}}{\varepsilon-\varepsilon_{L,res}} \tag{9a}$$

$$k_G=\begin{cases}0.4\beta_G^{\,3.6} & \beta_G\leq 0.64\\ \beta_G^{\,5.5} & \beta_G>0.64\end{cases}\qquad \beta_G=\frac{\varepsilon-\varepsilon_L}{\varepsilon} \tag{10}$$

The relative permeability model has proven to be well balanced between the level of detail (low) and the ability to capture the major hydrodynamic trends. However, it does

not make provision for partial wetting. Nemec & Levec (2005) showed that the assumption that $k_\alpha = k_{\alpha i}$ implies that the fluid-solid interfacial area in one phase flow and two phase flow is the same ($A_{\alpha S,1\text{phase}} = A_{\alpha S,2\text{-phase}}$), which can only be true when wetting efficiency is 1 and the liquid films are relatively thin. In such circumstances equation 9a can be derived theoretically to read:

$$k_L = \delta^3 \tag{11}$$

The power of the saturation (3) is close to the empirical value of 2.9. However, the same argument can be applied to the gas phase relative permeability and neither part of equation 10 corresponds. Levec et al. (1986) also suggested that altering the power in equation 9a from 2.9 to 2 gave a satisfactory correlation for the Levec mode. This issue will be returned to in section 2.3.2.

Closely related to the relative permeability concept is the F-function concept (Fourar et al., 2001). Starting from equation 6a, velocity is multiplied by a factor F_α to yield:

$$\left(-\frac{\Delta P}{\Delta z}+\rho_\alpha g\right)_{2-\text{phase}} = \frac{C_1 \mu_\alpha F_\alpha U_\alpha}{D_h^2} + \frac{C_2 \rho_\alpha \left(F_\alpha U_\alpha\right)^2}{D_h} \tag{12}$$

This approach is equivalent to the relative permeability approach for conditions of low effective velocity ($F_\alpha U_\alpha$), in which case $k_\alpha = 1/F_\alpha$. Interestingly, Fourar et al. (2001) then proceeds to make a case for the expression $F_\alpha = 1/\beta_\alpha{}^2$ which is valid for flow in a cylinder (Bacri et al., 1992) and which also happens to correspond to Levec et al. (1986)'s expression for the Levec mode. Unfortunately, Fourar et al. (2001) did not report their exact start-up procedure.

Slit Models

An extensive review of slit model approximations is given in Iliuta & Larachi (2005). Holub et al. (1992) postulated that gas-liquid trickle flow in a randomly packed bed behaves analogously to one-dimensional gas-liquid flow in an inclined slit. Writing

equation 4 for the slit for steady, non-interpenetrating fully wetted flow yields an expression that equates the pressure drop over a length of slit to the gas-liquid and liquid-solid shear stresses, which are in turn expressed as functions of the slit geometry and phase velocities in the usual Ergun (1952) formulation. They key to the slit approach is that the geometry of the slit can be mapped to the packed bed characteristics (namely the liquid holdup are related to the film thickness, the slit and the bed have the same solid surface area-to-volume, void-to-volume and liquid-to-solid volume ratios; pressure drop and the inclination angle is associated with the bed tortuosity or Ergun constants). Al-Dahhan et al. (1998) later extended the single slit model to account for discontinuities in the velocity and shear stresses at the gas-liquid interface (which introduces three additional empirical parameters – the velocity, f_v, and shear, f_s, slip factors and the interfacial liquid velocity). To account for partial wetting, Iliuta & Larachi (1999) introduced the double slit model that corresponds to the extended slit model together with a completely dry slit. The wetting is associated with the ratio of wetted slits to total slits. Its estimation requires another constitutive relation relating wetting efficiency with holdup and pressure drop. This can be attained from solving the liquid velocity profile in the wet slit in order to get an average velocity (Iliuta et al., 2000). This in turn is related to the other hydrodynamic parameters through a momentum balance (not unlike the Hagen-Poisseuille derivation). This then represents the state-of-the-art slit model approximation for co-current trickle flow (Iliuta & Larachi, 2005) and reduces to the other forms for a choice of simplifying assumptions (for example it reduces to Holub et al. (1992) single slit model for the assumptions of full wetting and no gas-liquid interaction, i.e. $f_s = f_v = 0$). As an interesting aside, there is a direct way of calculating the gas-liquid interfacial area from this kind of model, since it is directly proportional to the wetting efficiency. The generalized model equations are available in Iliuta et al. (2000) and are not repeated here. Additional refinements to the model were made by Iliuta et al. (1998), Iliuta et al. (2002a) and Iliuta et al. (2002b). Hydrodynamic multiplicity effects have not been incorporated into the general slit model.

Fundamental Force Balance

Tung & Dhir (1988) started from equation 5 but considered all the vertical force components acting on each phase for the geometry of two-dimensional film flow over a sphere (illustrated in Figure 9b). The force components are shown in Figure 9b. The force by which the gas pushes onto the particle through the liquid and the force by which the liquid pushes onto the particle (and their equal and opposite reactions) each have an interfacial drag and a pressure drag component. Note that here again complete wetting is assumed. Unsurprisingly, each force component is expressed in the Ergun formulation as the sum of viscous and inertial contributions. However, there are some subtleties to these formulations. For example, for the particle-gas drag the "diameter" of the particles are the sum of the particle diameter and the film thickness. Also, in expressing the gas-liquid interfacial force, a reference velocity at the gas-liquid interface has to be defined in order to account for slip. This is the same issue faced in the extended slit model formulation. Here, the reference velocity is taken as the saturation weighted average velocity. As before, the two Ergun constants appear in the equations. Attou et al. (1999) provided an equivalent derivation with the additional assumption that the tortuosity of each phase is inversely proportional to its holdup. Tung & Dhir (1988), Attou et al. (1999) and later Narasimhan et al. (2002) tested versions of this model for a miscellany of data produced by other investigators (including high pressure operation) and found it to be both accurate and robust.

Lattice-Boltzmann Simulation

The lattice-Boltzmann method is in principle a finite difference computational scheme of the Boltzmann equation. The Boltzmann equation describes the time evolution of a single-particle distribution in terms of a collision operator (Chen et al., 1994). The collision operator is in turn approximated by a single-time-relaxation process (with a relaxation time proportional to the kinematic viscosity). The particle distribution evolves toward an equilibrium distribution. Now, appropriately specifying the equilibrium distribution and taking the low flow velocity limit results in the method yielding a

computationally effective approximation of the incompressible Navier-Stokes equations (Chen et al., 1994). The lattice-Boltzmann method has been successfully applied to a variety of flow problems, including reactive flows in packed beds (Sullivan et al., 2005) and multi-phase hydrodynamics in packed beds (Manz et al., 1999, Gladden et al., 2003b), but excluding any hydrodynamic multiplicity effects.

Pore-Network Models

An alternative approach toward modelling trickle flow hydrodynamics is in viewing the void space in a packed bed as a set of interconnected pores bounded by the solid surface and the "pore necks" or constrictions, which can be thought of as the pore entrances and exits. Various definitions exist for defining these pore-to-pore connections and we will return to the issue in detail in Chapter 6. For the present discussion, it is sufficient to conceptualize the packed bed as an ensemble of pores such as the one depicted in Figure 9c (from Melli & Scriven, 1991). The pore itself is a capacity for which the gas and liquid competes (the pore therefore has a liquid holdup). Pressure drop due to drag forces are generally assigned to the pore-necks, who themselves can be occupied by gas, liquid or a combination of the two. Chu & Ng (1989) considered the pore structure of a tilted cubic packing of spheres. Each pore therefore has a coordination number of 6, i.e. six entrances/exists. The pore-to-pore connections are assumed to be cylinders with a length of 95.6% of the particle diameter. Their diameters are randomly assigned such that the diameter size distribution matches a computer-generated constriction size distribution generated in Chan & Ng (1988). The geometry thus set, it is further assumed that only four types of flow can occur in the cylinders: gas-phase gravity-viscous flow, liquid phase gravity-viscous flow, annular liquid-gas flow (for the film flow in the Kan-liquid mode) and stratified gas-liquid flow (for rivulet flow in the Levec mode). The final assumption is what is sometimes referred to as occupancy statistics, namely that a gas-liquid filled channel becomes completely liquid-filled when 86% of the cross-section is liquid filled (i.e. high channel holdup). An important additional observation is that because of the assumed symmetries, the liquid distribution is always regular, i.e. when

the liquid is to be divided at a pore exit into, say, 3 new channels, each channel takes one third of the flow rate.

Melli & Scriven (1991) used many of these concepts in the development of their pore-network model. However, they identify four types of bonds (instead of the four flow types in the cylinders of Chu & Ng, 1989), namely gas-continuous, liquid-continuous (flooded), liquid-bridged (no gas flow) and bubbling (gas bubbles in liquid flow). The sites (pores) have two variables, namely the volume of liquid in it and the pressure. Bonds (necks) have four variables: liquid saturation, liquid flow rate in and liquid flow rate out and the gas flow rate. The authors now introduce various *allowability* and *accessibility rules*. For example, a gas-continuous bridge is *allowed* to become a bubbling bridge if both the saturation and the liquid flow rate exceed pre-specified values. This does not mean that it necessarily will do so. To do so, either site connected to the passage must be *accessible* to the gas-continuous regime. Similar rules exist for all the other types of bonds. The issue of liquid distribution is again paramount. The authors assumed that when the liquid is faced with distributing to more than one passage, each passage gets a random fraction of the total flow (all the fractions adding up to 1). The drag terms in the passages are again taken as fully-wetted gravity-viscous flow in an assumed geometry of a bi-conical tube. This pore-network model is based on a thorough evaluation of the types of multi-phase flow that is encountered in porous media and makes a powerful argument that the macro-scale flow regimes are rooted in micro-scale phenomena. There are, however, two major drawbacks:

- It has a high level of complexity, which makes it both difficult to use (little or no follow-up work has followed its introduction) and difficult to validate experimentally (which has not been done). Extracting bed-scale trends that correspond to those in literature is relatively easy given the various aspects of the model that can be altered to do so. The model has not been applied to three-dimensional networks (possibly also because it would be computationally extraneous to do so).

- It has empiricism on multiple levels, including the specification of the allowability rules' critical values and the characteristics of the process by which the liquid is randomly distributed among potential outflow passages. Both of these drastically affect the calculated results and there is no fundamental way to specify them.

Another concern is that the level of detail with regards to the types of flow bonds and how they are created is not matched by an equivalent level of detail in the modelling of the drag forces in the assumed geometry of a bi-conical tube (for example, only viscous contributions are considered). It has not been tested how this latter assumption affects the results. In summary, while the model shows ample promise in capturing the micro-scale hydrodynamics, there are several critical issues that need further development. Its ability to capture multiplicity trends will be evaluated in section 2.3.2.

Computational Fluid Dynamics (CFD)

The computational fluid dynamics approach attempts to solve the volume averaged Navier-Stokes equations for two fluids. Drag forces are again expressed in the Ergun formulation with the difference in interstitial phase velocity as the characteristic velocity (U), full wetting again being assumed (Jiang et al. 1999). Ideally, the entire packed structure should be specified as the geometry (with boundary conditions imposed on every solid surface). This is computationally impossible at present. Instead, a meso-scale (cluster of particles) is viewed and it is then assumed that within such a meso-cell the porosity and holdup is uniformly distributed (Jiang et al., 1999). The cells are then randomly distributed throughout a two-dimensional bed in a way that ensures that the porosity distribution of the model bed matches that of an experimentally determined real packed bed. Constitutive mass and momentum balances are then solved in this geometry, usually by using a commercial CFD package. Propp et al. (2000) reformulated the mass and relative permeability-based momentum balances of Saez & Carbonell (1985) in terms of the total velocity (the sum of the gas and liquid velocities), yielding a one-dimensional

CFD model. The authors then proceed to give extensively detail on how to solve the resulting expressions numerically using the finite volume approach. Souadnia & Latifi (2001) applied this model (using a commercial CFD code) and showed that it agreed well with a limited set of experimental data. Gunjal et al. (2005) adopted Attou et al. (1999)'s formulation of the drag forces and Jiang et al. (1999)'s model two-dimensional bed and investigated various aspects of the model (including hysteresis and periodic flow). At present, indications are that CFD can develop into a powerful computational tool to represent hydrodynamics on the meso-scale. There are however, some areas of concern. Most notably is the fact that while the internal phase dynamics are modelled with relative ease, the boundary conditions are not (Dudukovic et al., 2002). This is termed the *closure problem* and introduces a significant amount of empiricism into the model (something that CFD was specifically trying to avoid). This is one reason why the 2D *model* bed is necessary. It is decidedly unclear whether this representation is valid, since once again there are many aspects to the model that can be tuned to yield results that match the limited experimental data on flow distribution. CFD in its present form deals with fully wetted beds, although hysteresis is dealt with by incorporating wetting efficiency in an empirical fashion (section 2.3.2). CFD's potential to be extended to the particle-scale will be evaluated in Chapter 6 in the context of new tomographical particle-scale imaging.

Other Approaches

Notable exceptions to the approaches summarized above are:

- The *partially-wetted particle model* (Zimmerman & Ng, 1986). These authors constructed a model 2D bed by dropping particles (disks) into a rectangle with liquid then introduced to the top layer. Liquid flows from sphere to sphere through contact points and the total flow rate to a sphere determines its degree of wetting (according to a de-wetting criterion, Ng, 1986). The model is similar to a pore-network except that spheres instead of pores are chosen as fundamental unit. The model has not seen further development, except in the conceptual interpretations of Maiti et al. (2005).

- Holub (1990) introduced the discrete cell model (DCM), where the minimum rate of mechanical energy dissipation is the governing principle and the bed geometry is the same as the one used for CFD calculations. Jiang et al. (1999) extended the approach to incorporate capillary pressure and showed that it agreed well with the results of the CFD approach for the same assumed geometries. Hysteresis is dealt with in the same manner as in the CFD approach (section 2.3.2). One major advantage of DCM is that it offers a good balance between the ease by which problems are formulated and the level of detail regarding the flow pattern that can be extracted from it.
- Several conduit models have been proposed (Biswas et al., 1988, Saez et al., 1986, Pironti et al., 1999 and Boyer & Fanget, 2002). The basis of these models is that the flow in a packed bed can be represented as a bundle of vertical tubes that can be straight or constricted. The drag forces in equation 5 are expressed in terms of an actual (interstitial) velocity and a hydraulic diameter. Another form of this model is the multi-zone model of Wang et al. (1995), where the bed is divided into gas-filled, liquid-filled and two-phase flow zones. The relative fractions of flow assigned to each of these zones are indicative of the flow uniformity. However, the model is not predictive since there is no way to determine these fractions a priori.

2.3.2 Hydrodynamic Multiplicity Modelling

Not all of the approaches discussed above have been extended to include the impact of hydrodynamic multiplicity. That hydrodynamic multiplicity is a neglected issue in hydrodynamic modelling is apparent from an evaluation of the hydrodynamic literature for approximately the last 3 decades (as reported in Dudukovic et al., 2002). Of the 28 recommended pressure drop and holdup models, none can deal with the issue of hydrodynamic multiplicity. This is a major concern for two reasons:

- Form an academic point of view, it does not make sense to model path variables as state-variables. Models that take only one hydrodynamic mode into account can at best succeed in predicting only that one mode. However, it is desirable to have a single mathematical framework by which all modes (and the states in-between modes) can be treated and where the distinction is based on a fundamental physical principle.
- Form an application point of view, there are a plethora of hydrodynamic states with different hydrodynamic characteristics that remain unexplored. Since hydrodynamics has a significant impact on the performance of the reactor, filter or absorption column, the different hydrodynamic options presented by multiplicity can be exploited to yield optimum performance.

An argument that is often aired as to why hydrodynamic multiplicity is relatively unimportant, is that the Kan-Liquid mode is the obvious optimum. This is based on the idea that since it has the highest pressure drop of all the modes (and therefore the highest degree of gas-liquid interaction), it must be the optimum. This is true for gas-liquid mass transfer limited systems, which are widely found, but there is no reason to believe that this mode must be the optimum for other equally common applications (like liquid-solid mass transfer limited systems). A hint that it might not be is the fact that the Kan-Gas mode has a higher holdup (and therefore presumably a higher wetting efficiency) than the Kan-Liquid mode. The idea of a hydrodynamic optimum is explored in Chapter 8.

Some of the approaches alluded to above have been extended to incorporate some aspects of hydrodynamic multiplicity. These are summarized in Table 9 and are discussed next.

Kan & Greenfield (1978) studied the evolution of a Kan-Liquid mode into a Kan-Gas mode with gas velocity changes. Later (Kan & Greenfield, 1979), they adopted the Turpin & Huntington (1967) empirical pressure drop model and introduced a maximum gas flow rate Reynolds number to account for the lower pressure drop in the modes between the Kan-Liquid and Kan-Gas modes. The model does not consider holdup. They

also speculated that the increased gas flow reduced the gas flow path tortuosity and then quantified this reduction. The empirical nature of this model makes it undesirable. In particular, one needs 9 fitted parameters for the Kan-Liquid mode, as well as another one that has to be introduced when gas velocity changes are used.

Table 9. Hydrodynamic multiplicity modelling in literature

Reference	Approach	Comments
Kan & Greenfield (1979)	Empirical	Deals only with gas flow rate variation induced hysteresis, but not just for the limiting cases. Highly unsatisfactory because of the high degree of empiricism.
Levec et al. (1986)	Relative permeability	Deals only with Levec and Kan-Liquid/Super modes. Multiplicity introduced externally by specifying a different permeability correlation. Predicts holdup well at low u_L.
Chu & Ng (1989)	Pore-network	Deals only with liquid flow rate variation induced hysteresis. Multiplicity introduced by externally specifying flow type. Good predictive capability.
Melli & Scriven (1991)	Pore-network	Very complex model. Applied to liquid flow rate variation induced hysteresis only. Multiplicity emerges naturally from flow history. Highly empirical. Not validated.
Wang et al. (1995)	Multi-zone model	Not predictive, but rather indicative of extent of flow uniformity.
Jiang et al. (1999) Gunjal et al. (2005)	CFD and DCM	Only meso-scale 2D beds. Deals only with non-pre-wetted and "pre-wetted" beds. Wetting and hysteresis introduced empirically through capillary pressure. Under-predicts multiplicity.

Levec et al. (1986) suggested that hysteresis is due to the differences in advancing and receding contact angles (increasing liquid flow rate legs being associated with advancing contact angles and decreasing legs with receding contact angles). Receding contact angles are lower, implying more liquid spreading. However, Levec et al. (1986) adopted the relative permeability approach and introduced hysteresis into the power of the liquid phase relative permeability. Whereas equation 9a accounts for the Kan-Liquid (and Super) modes, a new equation is introduced for the Levec mode (the power of the saturation being 2):

$$k_L = \delta^2 \qquad (9b)$$

This equation is especially valid for low velocities and cannot account for the states in-between the Levec and Kan-Liquid modes. Since this model is the only practical alternative for obtaining quantitative predictions for the Levec mode, it is informative to plot the model's performance for the original data (Figure 10). Note that for the Levec mode satisfactory predictions are only achieved at low liquid velocity – at higher velocities (u_L > 10 mm/s) the functional dependency is clearly different from the adopted power law expression. At the pulsing boundary (u_L ≈ 18 mm/s) the holdup is equal in both modes but the correlation still predicts a large difference. Evidently, the gas phase relative permeability-gas saturation relationship also needs adjustment in the Levec mode.

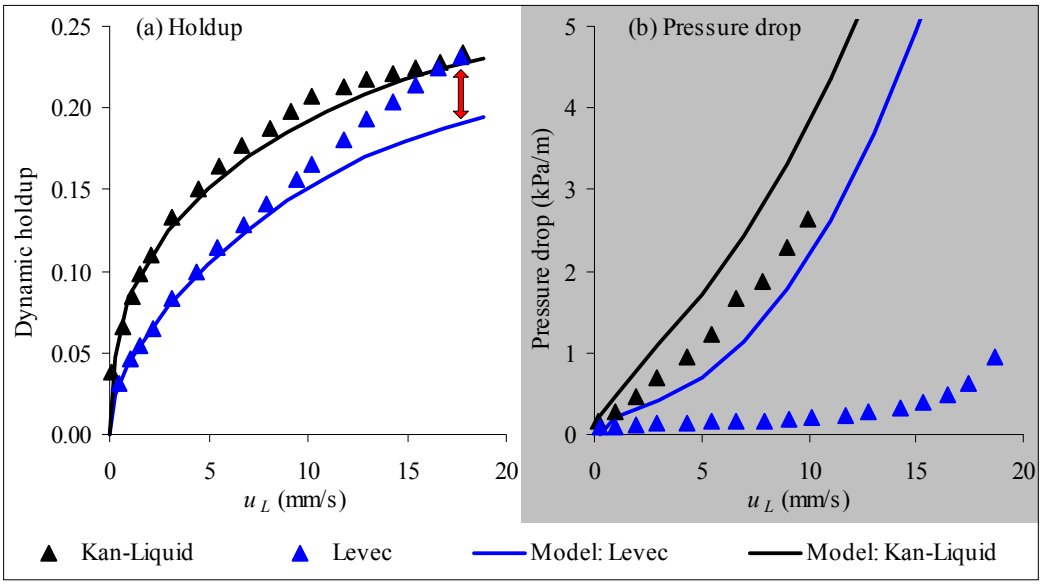

Figure 10. The inapplicability of the power law form for the Levec mode's permeability-saturation relationship at high u_L. Model and data from Levec et al. (1986).

Chu & Ng (1989) introduced hysteresis in their pore-network model by assuming that the cylinders that connect pores are in the annular flow regime for the Kan-Liquid mode and in the stratified flow regime for the Levec mode. Although the authors state that these two regimes correspond to film and rivulet flow, there seems to be little physical basis for

these assumptions. Melli & Scriven (1991) also showed that their pore-network model exhibits hysteresis with liquid flow rate. The hysteresis is derived from the fact that the allowability and accessibility criteria are asymmetrical with flow rate (they are functions of saturation among other things). The result is that different bond types prevail depending on whether the flow is increasing or decreasing. Although the criteria are set empirically, they are not changed according to the mode (i.e. the empirical part is the same for both the Non-pre-wetted and Kan-Liquid modes). This is the only hysteresis model that has this quality. To re-iterate, for an increase in liquid flow rate, the local pore saturations increase. As liquid flow rate is decreased, the high saturations allow different types of bonds (bubbling and flooded) to persist at the reduced flow rate where they were impossible before. This results in the observed liquid flow rate variation induced hysteresis. This mechanism has not been tested for gas flow rate variation induced hysteresis (Kan-Gas mode), nor for pre-flooding under irrigation (Super mode).

As mentioned before, Wang et al. (1995) conceptually divided the bed into three zones and showed that the different modes correspond to different fractions of flow in each of the modes. Again, there is no a priori method of determining these fractions for the different hydrodynamic conditions.

The CFD approach has seen attempts to extend it to incorporate hysteresis. Jiang et al. (1999) suggested that an empirical wetting efficiency be incorporated into the capillary pressure expression:

$$P_G = P_L + P_C\left(1 - f\right) \tag{13}$$

The capillary pressure (P_C) can be formulated as suggested by Grosser et al. (1988). The expression reduces to the absence of capillary pressure when the wetting is complete ($f = 1$). Jiang et al. (1999) suggested that the wetting be set to zero for Non-pre-wetted beds and one for pre-wetted beds (no distinction is made between Levec, Kan-Liquid, Kan-Gas or Super modes). Both the CFD and DCM models exhibit liquid flow rate variation induced hysteresis under this assumption. Gunjal et al. (2005) also adopted

equation 13 and compared CFD predictions to their own pressure drop and holdup liquid flow rate variation induced hysteresis data. While the trends are qualitatively represented, they found that the extent of hysteresis for both parameters were severely under-predicted (the Non-pre-wetted mode pressure drop is over-estimated). Considering that *f* is taken as either 0 or 1, it an be concluded that this assumed capillary effect *as formulated* cannot alone explain hysteresis. Moreover, the framework allows no way of dealing with gas velocity variation induced hysteresis. Assuming full wetting for pre-wetted beds and zero wetting for non-pre-wetted beds is a questionable practice.

Using the advancing/receding contact angle idea, Khanna & Nigam (2002) and later Maiti et al. (2005) presented an in depth analysis of spreading dynamics on porous and non-porous surfaces and conclude that hysteresis (liquid flow rate variation induced) is attributable to the concept of participating and non-participating particles. At low velocity, the liquid flows predominantly in "favourably clustered" particles. As the flow rate is increased, the liquid spreads out from this core. A subsequent decrease results in previously non-participating particles now also participating. The idea is reminiscent of that of Christensen et al. (1986) who visualized the Levec mode as consisting of liquid-filled cores surrounded by film flow. Interestingly, tomographical techniques can be used to validate these ideas. Sederman & Gladden (2001) reported that the number of rivulets increased as the liquid velocity is increased in the Levec mode. At higher velocity the number of rivulets did not increase but the rivulets instead swelled. In their analysis, the Kan-Liquid mode had more rivulets than the Levec mode, suggesting that more particles participate. However, it is possible to literally count the number of participating particles by tomographical means and this has not been done. This issue is returned to in Chapter 6, where it is posed that the number of participating pores is a better evaluation. The Maiti et al. (2005) framework does not account for gas flow rate variation induced hysteresis.

In the early stages of this study, Van der Merwe & Nicol (2005) adopted the conduit flow model of Boyer & Fanget (2002) and incorporated a "volumetric utilization coefficient"

into the drag force terms. This is equivalent to conceptually partitioning the bed into two regions: one that experiences fully wetted liquid flow and another that experiences no liquid flow. The only notable aspect of this model is the fact that (unlike other hysteresis models) the utilization coefficient can be determined independently as the residual holdup utilization. As such, it is a measure of the degree of spreading of the liquid in the bed. Using this coefficient, we were able to predict the holdup in the Non-pre-wetted, Levec and Super modes for the case of no gas flow (and a limited data set). The model is yet to be extended to pressure drop prediction and needs further validation.

2.3.3 Outstanding Issues

One major unresolved issue that has in fact received only empirical and statistical attention is the issue of the *mechanism of liquid distribution* and how this results in different hydrodynamic modes. It is generally well established that the different hydrodynamic modes are associated with different gas and liquid flow patterns. However, there has been little speculation and even less evidence as to how these flow patterns come about. Levec et al. (1986) suggested that the multiple states are the result of the hysteresis in the gas-liquid-solid contact angle when a liquid front is advancing and receding over the particle surfaces. Wang et al. (1995) associated the multiplicity with non-uniformity and developed a multi-zone model that measured this post priori. Van der Merwe & Nicol (2005) used the same idea, but quantified the uniformity in terms of a residual holdup utilization. Jiang et al. (1999) attributed hysteresis to differences in the capillary pressure expression. Maiti et al. (2005) ascribed it to the fraction of participating and non-participating particles but gave no indication of how this should be determined. This begs the question: *What is the fundamental mechanism that causes hydrodynamic multiplicity and how should it be incorporated into the already successful phenomenological models?*

2.4 Conclusions

The following conclusions are drawn from the literature evaluated in this chapter:

- **Hydrodynamics are difficult to model** owing to the complexities of gas-liquid-solid interactions, but not as difficult to understand qualitatively. This is evident in that the basic trends are more or less intuitive (for example, a higher liquid flow rate yields a higher holdup and therefore higher pressure drop). As a result, there are numerous different phenomenological approaches that attain a fair measure of success. Hydrodynamic multiplicity, however, is far less intuitive, has not received as much attention and is relatively poorly understood.
- **The hydrodynamic parameters are *all* influenced by hydrodynamic multiplicity and the extent of variability is large.** Adopting the modes interpretation introduced herein, it is clear that no single investigator studied all the modes (see Table 7). Also clear is the fact that the hydrodynamic behaviour is very complex, i.e. that different hydrodynamic states can be achieved in different ways (pre-flooding and/or hysteresis) and that the modes are different in character (flow pattern, liquid morphology and interfacial areas). The lack of an experimental framework that incorporates all the various combinations of pre-wetting and flow rate changes has led modellers to consider only some aspects of the phenomenon. This is a question of problem definition and is addressed as the first objective of this work.
- **It is unclear what the root cause of hydrodynamic multiplicity is.** Suggested mechanisms include contact angle hysteresis (Levec et al., 1986), the dynamics of a spreading film over porous/non-porous substrates (Maiti et al., 2004), flow uniformity (Wang et al., 1995), participating and non-participating particle clusters (Maiti et al., 2005), imperfect wetting (Lazzaroni et al., 1988), the flow differences between rivulet and film flow (Christensen et al., 1986) and the change in tortuosity of the gas channels (Kan & Greenfield, 1979).

- **Hydrodynamic models do not capture multiplicity trends.** Those that have attempted to incorporate multiplicity have generally done so for only one of the two manifestations thereof (namely liquid flow rate variation induced hysteresis loops and pre-wetted vs. non-pre-wetted modes). Moreover, multiplicity has only been incorporated into models *empirically* and with little quantitative success.

However, considerable experimental work has been done on this topic. Returning to Figure 1, note that a major objective of evaluating the literature was to identify characteristic multiplicity trends with the aim of providing a basis from which the proposed fundamental mechanism can be tested. These trends are:

(A) There are different flow patterns in the different modes: rivulet-type flow in the lower limiting cases and film-type flow in the upper limiting cases. New rivulets are created as u_L increases.

(B) Liquid flow rate variation induced hysteresis causes increases in pressure drop and liquid holdup in the Non-pre-wetted and Levec modes.

(C) Gas flow rate variation induced hysteresis causes increases in pressure drop and holdup in the Levec mode, but an increase in holdup and a decrease in pressure drop in the Kan-Liquid mode.

(D) The extent of pressure drop hysteresis is diminished when particle size is increased.

(E) The Levec mode *wetting efficiency* is lower on average and shows a bi-modal particle wetting distribution, whereas the Super mode shows a Gaussian distribution.

This list will be extended and modified throughout the remainder of the experimental investigations (Chapters 4, 5, 6 and 7).